Leary, R.J., Umhoefer, P., Smith, M.E., Smith, T.M., Saylor, J.E., Riggs, N., Burr, G., Lodes, E., Foley, D., Licht, A., Mueller, M.A., and Baird, C., 2020, Provenance of Pennsylvanian–Permian sedimentary rocks associated with the Ancestral Rocky Mountains orogeny in southwestern Laurentia: Implications for continental-scale Laurentian sediment transport systems: Lithosphere, https://doi.org/10.1130/L1115.1.

GSA Data Repository Item 2020103

Provenance of Pennsylvanian-Permian sedimentary rocks associated with the Ancestral Rocky Mountains in Southwestern Laurentia: Implications for continental-scale Laurentian sediment transport systems

Ryan J. Leary[1], Paul Umhoefer[2], M. Elliot Smith[2], Tyson Smith[3], Joel Saylor[3], Nancy Riggs[2], Greg Burr[2], Emma Lodes[2], Daniel Foley[2], Alexis Licht[4], Megan Mueller[4], Chris Baird[4]

[1]Department of Earth and Environmental Science, New Mexico Institute of Mining and Technology, Socorro, NM 87801

[2]School of Earth and Sustainability, Northern Arizona University, Flagstaff, AZ 86011

[3]Department of Earth and Atmospheric Sciences, University of Houston, Houston, TX 77204

[4] Department of Earth and Space Sciences, University of Washington, Seattle, WA 98195

Sample Locations

Sycamore Canyon (Arizona Shelf; supplemental Fig. 1)

Location and Lithofacies

This section is exposed WNW of the town of Sedona, Arizona. It consists of Mississippian through middle Permian rocks, and the section has not been substantially affected by basin and range extension. Mississippian Red Wall Limestone makes up the base of the section, and above this Supai Group, Hermit Formation, and Schnebly Hill Formation make up the sampled section (Blakey, 1990).

The Supai Group (sensu Blakey, 1990) at this location is subdivided into a lower Undivided section and the upper Esplanade Sandstone, interpreted to be equivalent to the Esplanade Sandstone as defined in the Grand Canyon (McKee et al., 1982). The basal Undivided Supai Group at this location consists of a poorly exposed chert granule conglomerate in disconformable contact with Mississippian limestone. Above this, the section consists of ca. 60 m of laterally extensive, tabular, very fine- to fine-grained, horizontally laminated sandstone beds with sparse ripple cross-lamination and weak paleosol development (Supplemental Fig. 1). Roughly 90 m of horizontally laminated and planar cross-stratified fine-grained sandstone interbedded with very fine-grained, mottled, nodular calcic sandstone; bioturbation and rhizoliths are common within these sandstones. Many fine-grained sandstones within this interval show bleached tops. Above this interval is ca. 55 m of horizontally laminated and planar cross-stratified fine-grained sandstone with foresets ranging between 0.2 m and >1 m in height. This interval is interpreted lithologically equivalent to the Esplanade Sandstone of Grand Canyon Strata (Lane, 1979; McKee et al., 1984; Blakey, 1990). The Esplanade Sandstone is overlain by ca. 230 m of dominantly very fine-grained, horizontally stratified and massive sandstone interbedded with massive calcic sandstones and sparse silty calcic paleosols. This interval also contains several incised rounded pebble conglomerates. Blakey (1990) interprets this interval as the equivalent to

the Hermit Formation although it contains substantially less mudstone than the Hermit Formation as defined within the Grand Canyon section (McKee et al., 1982). The Hermit Formation is overlain by the Schnebly Hill Formation (Blakey, 1990), which consists here of ca. 165 m of very fine-grained to fine grained horizontally stratified, trough cross-bedded, and planar cross-bedded sandstones. Trough cross-strata foresets range from ca. 0.5 m to 1 m in height whereas planar cross-strata foresets are ca. 1-6 m in height. Adhesion structures are common within this interval (e.g. Kocurek and Fielding, 1982). Clay and silt-sized material is almost entirely absent from this formation. The boundary between the Hermit Formation and the Schnebly Hill Formation is transitional (Supplemental Fig. 1), but is marked by a major color change and the occurrence of >1 m scale planar cross-stratification.

Age

Age determinations for this section are based on lithostratigraphic correlation. The Undivided Supai Group is interpreted as Pennsylvanian in age based on stratal relationship to the Horquilla Limestone in southern Arizona (Ross, 1973), early Pennsylvanian brachiopods in Chino Valley, 40 km southwest of Sycamore Canyon (Hughes, 1952), correlation of limestone intervals with Grand Canyon Strata (McKee, 1982), and Atokan-Virgilian fusulinids at a section ca. 230 km to the northeast (Blakey, 1990).

The Esplanade Sandstone is interpreted as early Permian (Wolfcampian) in age based on an interfingering relationship with the fossiliferous Pakoon Limestone in the Grand Canyon (McKee, 1982).

The overlying Hermit Formation is interpreted here as early Permian (Wolfcampian age) based on its stratigraphic position below the Fort Apache Limestone (see below) and lithostratigraphic correlation to the Hermit Formation in the Grand Canyon (Blakey and Knepp, 1989; Blakey, 1990) where it was dated based on plant fossils (White, 1929).

The Schnebly Hill Formation is interpreted as Middle Permian (Leonardian) in age based on molluscan fauna (Winters, 1963) and conodonts (Weisman, 1986; Blakey, 1990) collected from the Fort Apache Limestone, which cuts the Schnebly Hill Formation along the Mogollon Rim east of Sedona. This section is capped by the Coconino Sandstone, interpreted to be late Leonardian in age based on its stratigraphic position above the Fort Apache Limestone and Schnebly Hill Formation (Blakey, 1990).

Depositional Systems

The Lower Supai Group (undivided) is interpreted as the remnants of a mixed terrestrial-marine depositional setting (e.g. Blakey, 1990). The basal series of chert pebble conglomerates are interpreted to represent high energy fluvial deposition above a subareial exposed karst surface atop the Redwall Limestone. Above this, very fine- to fine-grained horizontally laminated sandstones interbedded with weakly developed paleosol horizons that include rhizoliths are interpreted to represent a nearshore terrestrial environment (Blakey, 1990). Poorly preserved marine fossils and limestones within the Supai Group exposed west of this section (Hughes, 1952) as well as numerous marine limestones within the Supai Group exposed in the Grand

Canyon (McKee, 1982) support this conclusion. The Esplanade Sandstone is interpreted as a principally coastal dune deposit that includes shallow marine, esturatine, and eolian strata (McKee, 1982; Blakey, 1990). In the Sycamore Canyon section, >1 m scale planar cross-bedding, horizontal stratification, and minor eolian adhesion structures of the Esplanade Sandstone are interpreted as eolian with some peritital influence (Blakey, 1990). Above this, the Hermit Formation is interpreted as fluvial deposit with abundant flood-plain and coastal plain deposits (Blakey and Knepp, 1989; Blakey, 1990). The Schnebly Hill Formation in this section was deposited in the western Holbrook Basin (Blakey, 1990) and eolian, limestone, and evaporitic facies are regionally is interpreted to represent deposition within a restricted marine to sabkha environment (Blakey and Middleton, 1983; Blakey, 1990). Marine limestone of the Fort Apache Member (or Limestone) pinch out west of the Sycamore Canyon section, and the Schnebly Hill facies present at this location are interpreted as eolian deposits.

Plomosa Mountains (Arizona Shelf; supplemental Fig. 2)

Location and Lithofacies

We collected samples from the Supai Group, Hermit Formation, and Coconino Sandstone exposed southern Plomosa Mountains in western Arizona southeast of the town of Quartzite. These rocks exposed in a steeply dipping, fault bounded panel within a zone that has been subjected to multiple episodes of intense compressional and extensional deformation (Miller, 1970; Richard et al., 1992; Richard, 1993; Richard et al., 1993; McQuarrie and Wernicke, 2005; McQuarrie and Oskin, 2010; Spencer et al., 2015). Most late Paleozoic sedimentary rocks in this region have been intensely deformed and metamorphosed. The section sampled for this study is a rare exception and is preserved largely unmetamorphosed, although extensive desert varnish on most outcrops makes recognition of sedimentary structures difficult.

The Paleozoic succession in western Arizona qualitatively resembles the Paleozoic section preserved within the Grand Canyon and Mogollon Rim, and have been inferred to be equivalent strata (Miller and McKee, 1971; Richard et al., 1993). The Plomosa Mountains are currently ca. 200 km southwest of the mostly undeformed Sycamore Canyon section (above), but accounting for Basin and Range extension, this section palinspastically restores adjacent to the edge of the Colorado Plateau (McQuarrie and Wernicke, 2005).

The basal Supai Group equivalent rocks are deposited above an erosional surface on brecciated, white limestone interpreted as equivalent to the Mississippian Redwall Limestone (Supplemental Fig. 2, Miller, 1970; Richard et al., 2003). Above this, Supai Group equivalent rocks consist of ca. 50 m of red, dominantly horizontally stratified fine to coarse-grained calcic sandstone (Supplemental Fig. 2). Above this, red, fine-grained horizontally stratified sandstone is interbedded with beds of greenish-gray silty limestone. These facies transition into poorly exposed trough and planar cross-stratified sandstones. At the upper extent of Supai Group equivalent rocks, facies are dominated by horizontally stratified sandstones interbedded with red, massive and mottled mudstone-siltstone beds. Two prominent channelized, massive clast-supported pebble conglomerate beds are preserved above this. After 22 m of covered section, large-scale (> 2 m) planar cross-bedded sandstones of interpreted Coconino Sandstone equivalence crop out. Facies are interpreted to be equivalent to both the Hermit and Schnebly

Hill Formation are absent from this section, although the upper ca. 60 m of exposed strata below the Coconino Sandstone most closely resemble Hermit Formation facies at the Sycamore Canyon section.

Age

Stata within the Plomosa Mountains section have not been directly dated, and age determinations for this study are based on correlation with Sycamore Canyon, Grand Canyon, and Mogollon Rim strata. The basal Supai Group equivalent rocks are interpreted as Pennsylvanian, and strata directly below the Coconino Sandstone are interpreted as lower Permian. The Coconino Sandstone is interpreted to be age equivalent to the Coconino Sandstone along the Mogollon Rim and thus Leonardian in age.

Depositional Systems

This section is interpreted to have been deposited above an erosional disconformity on a karst surface developed on Mississippian limestone. The Supai Group equivalent rocks are interpreted to represent a continuation of the mixed marine-terrestrial depositional environment preserved in the Sycamore Canyon section (above). Extensive desert varnishing mostly precluded detailed examination and interpretation of sedimentary structures within Supai equivalent rocks. The presence of distinct limestone intervals within the middle of the Supai equivalent section suggests that this location was more marine dominated and thus in a more distal position than the Sycamore Canyon section. The upper portion of Supai equivalent rocks (2QZ, Supplemental Fig. 2) are interpreted to represent deposition within a fluvially dominated coastal-plain setting similar to strata preserved along the Mogollon Rim (Blakey and Knepp, 1989; Blakey, 1990). Large scale (>2 m) cross-bedded sandstones at the top of the section are interpreted as remnants of the same large eolian erg system (e.g. Blakey et al., 1988) that deposited the Coconino Sandstone in the Grand Canyon and Mogollon Rim regions.

Mogollon Rim (Arizona Shelf; supplemental Fig. 3)

Location and Lithofacies

This section is exposed along the Mogollon Rim escarpment northeast of the town of Payson, Arizona. The base of the Pennsylvanian-Permian section is deposited above a disconformable karst surface developed on the Mississippian Redwall Limestone (Huddle and Dobrovolny, 1945; McKee and Gutschick, 1969). A wide range of stratigraphic schemes have been proposed for this region, which is transitional between the siliciclastic dominated Pennsylvanian-Permian section to the northwest and the carbonate dominated Pennsylvanian section to the southeast (e.g. Huddle and Dobrovolny, 1945; Ross, 1973; Blakey and Knepp, 1989). Here, we use the stratigraphic naming scheme of Blakey and Knepp (1989) in which this section consists of the Pennsylvanian Naco Group (equivalent to the Horquilla Limestone of Southeast Arizona (Ross, 1973; Brew and Beus, 1976; Blakey and Knepp, 1989)) and the Permian Hermit Formation, Schnebly Hill Formation including the Apache Limestone Member, and the Coconino Sandstone.

Northeast of Payson, the Naco Formation consist of a series of grey fossiliferous limestones interbedded with red siltstones that become increasingly abundant upsection (Ross, 1973; Brew

and Beus, 1976). The Naco Formation sampled for this study is poorly exposed Northwest of Payson and consists of calcic horizontally stratified and trough cross-bedded sandstones, micritic mudstones, and pebble to cobble conglomerates composed of rounded grey limestone and massive red sandstones clasts (Supplemental Fig. 3, 5PS). Samples were collected from three horizontally stratified sandstone intervals within this section.

Above this, the Hermit Formation (Blakey and Knepp, 1989) or Amos Wash Member of the Supai Formation (Huddle and Dubrovolny, 1945; Winters, 1963; Pierce, 1989; Blakey, 1990) consists of ca. 250 m of poorly exposed red colored strata that are dominated by recessive siltstone and mudstone interbedded with thin (10-50 cm thick), tabular sandstones. Siltstone and mudstone intervals are mostly massive, often contain nodular calcite, and are often mottled with greenish siltstone and mudstone. Rare intervals are entirely green in color. Tabular sandstone beds typically have non-erosive bases and are laterally continuous for hundreds of meters. Sandstones of these beds are horizontally stratified or planar cross-stratified with minor current ripple cross-lamination also present (Supplemental Fig. 3). Two conglomeratic intervals occur in this section; both are clast-supported limestone pebble conglomerates.

The transition to the Schnebly Hill Formation or Big A Hill Member of the Supai Group (sensu Pierce, 1989) was not clearly identified in this study. The facies change from interbedded mudstones and channelized sandstones to tabular, horizontally stratified sandstone and mudstones that marks the base of the Schnebly Hill Formation at its type location (Blakey, 1990) is gradational at this location. However, in the upper Hermit Formation, there is an increase in average grain size, and the dominant facies becomes horizontally stratified, very fine-grained sandstone. Siltstone interbeds are much less abundant than within the Hermit formation, mottling within these beds is less common, and calcic nodules are almost entirely absent from this interval. Approximately 80 m above the transition into the Schnebly Hill Formation, the section consists of ca. 25 m of red mudstone and siltstone with prominent mottled, undulatory green bands (Supplemental Fig. 3). Above this, there is a major color change from dark red to tan-brown, ca. 5 m above which is the base of the Fort Apache Limestone Member (Stoyanow, 1936; Blakey and Knepp, 1989; Blakey, 1990). This interval consists of ca. 26 m of fossiliferous limestone, dolostone, and siltstone. Limestone/dolostone beds within this section are oncoidal wackestone, bioclastic wackestone, and wavy-laminated micrite; small brachiopods are common bioclasts (Supplemental Fig. 3). Interbeded with these intervals are massive, tan, silty micrites containing sporadic brachiopod fossils. Above this are strata of the Corduroy Member (Winters, 1963), which is included the Schnebly Hill Formation (Blakey and Knepp, 1989; Blakey, 1990). These rocks consist of two dominantly limestone intervals interbedded with red sandstone and siltstone. Sandstone beds typically consist of very fine-grained, horizontally stratified and massive beds <1 m thick interbedded with red, horizontally laminated or massive siltstones. Limestone intervals typically consist of yellow, green, and pink silty micrites with a few bioclastic wackestones that include fine shell debris and brachiopod fossils. Yellow, sparite-rich intervals are present in the lower of the two limestone intervals.

Whereas the transition between Schnebly Hill Formation facies and overlying Coconino Sandstone facies is abrupt in the Sedona area near where the Schnebly Hill Formation was defined (Blakey and Knepp, 1989; Blakey, 1990), the contact in this section is gradational. The upper part of the Schebly Hill Formation consists of red-orange fine-grained sandstone beds that include both meter scale planar cross-stratification and horizontal lamination. Many beds contain nodular carbonates and are bioturbated. Up-section, white sandstone increases in abundance at

the expense of red-orange sandstone and 1-2 m planar cross-stratification becomes the volumetrically dominant facies. The second most abundant facies in this interval is wavy laminated and wave-rippled sandstone. Above this, the unambiguous Coconino Sandstone facies are characterized by fine-grained, white sandstone with large-scale planar cross-strata; individual cross-sets are up to 10 m high. The youngest sample from this section included in this study was collected from the upper unambiguously Schnebly Hill Formation (Supplemental Fig. 3).

Age

Two intervals within this section provide robust age constraints. Fossiliferous limestones of the Naco Formation have been dated as Desmoinesian to Missourian (Brew, 1965; Brew and Beus, 1976), and conondonts collected from the Fort Apache Member of the Schnebly Hill Formation have been identified as Leonardian (Weisman, 1986; Peirce, 1989). Plant fossils from the Supai Formation above the Naco Group have been interpreted as Late Pennsylvanian to Early Permian, (Blazey, 1971; Pierce, 1979). Although many age/correlation problems persist for strata in this region (e.g. Peirce, 1989), biostratigraphic control from the Naco Goup and Fort Apache Member provide age constraints sufficiently precise for the time divisions used in this study.

Depositional Systems

The Limestones of the Naco Group are interpreted as the northwest distal extent of major marine transgressions within Pedregosa Basin to the southeast (Ross, 1973). Strata of this interval are interpreted to have been deposited within indistriubutary systems as well as lagoonal settings (Ross, 1973). The presence of red, nodular calcareous mudstones within this interval suggests periodic exposure and soil development occurred during middle-upper Pennsylvanian time (Kenny and Neat, 1993). Rocks of the Hermit Formation (sensu Blakey and Knepp, 1989) or Amos Wash Member of the Supai Formation (sensu Winters, 1963; Ross, 1973; Peirce, 1989) are interpreted to represent deposition in a delta-plain and/or fluvial distributary system (Blakey and Knepp, 1989). Rare conglomerates as well as planar and trough cross-stratified sandstones are interpreted as channel deposits (Blakey and Knepp, 1989). Above this, strata of the lower Schnebly Hill Formation (Blakey and Knepp, 1989; Blakey, 1990) or Big A Butte Member of the Supai Formation (Winters, 1963; Ross, 1973; Peirce, 1989) are interpreted to have been deposited within a Sabkha/tidal flat environment. Wavy laminated, wave ripple-cross laminated, and small (<1 m high) scale planar cross-stratified sandstones suggest periods of eolian deposition, deflation to the water table, and periods of submergence by shallow standing water (e.g. Kocurek and Day, 2018). Above this, large scale (up to 10 m high) planar cross-strata suggest the encroachment of a well-developed eolian system and a complete drying up of this area (Pierce et al., 1977; Blakey and Middleton, 1983).

Mescal Mountains (Central Arizona; supplemental Fig. 4)

Location and Lithofacies

This section is located ca. 140 km west-southwest of Phoenix, Arizona, just west of the San Carlos Reservoir. The section is fault-bounded and consists of ca. 375 m of strata mapped as Pennsylvanian Horquilla Limestone deposited conformably atop Mississippian Escrabrosa Limestone (Wrucke et al., 2004). This section is dominated by medium bedded (average 1-3 m) grey mustone and fossiliferous wackestone containing abundant crinoid stem and brachiopod fossils (Supplemental Fig. 4). Horizontal pink chert stringers are common within this section;

horizontal burrows are also present in some fossiliferous wackestones. In the upper section, three prominent massive, fusulinid-rich wackestones were sampled for age control. The only siliciclastic material identified and sampled in this section was from five meters of horizontally laminated, wavy bedded, and current ripple cross-stratified quartzose sandstone 241 m above the base of the section (Supplemental Fig. 4).

Age

Age control for this section is provided by fusulinid biostratigraphy performed by Greg Wahlman. Based on the presence (in ascending order for the three horizons sampled) *Triticites* cf. *cullomensis*, *Triticites plummeri*, and *Schwagerina* aff. *dunnensis*, the interval from which the detrital zircon sample was collected is interpreted as Late middle Virgilian to latest Virgilian (Dunbar and Condra, 1927; Myers, 1958; Sabins and Ross, 1963; Kauffman and Roth, 1966). See included biostratigraphic report for more detail.

Depositional Systems

This section interpreted to have formed within a low to moderate-energy shallow carbonate shelf environment (Ross, 1973) with little siliciclastic input. This suggest that during the Pennsylvanian, the limit of substantial siliciclastic input to central Arizona marine systems was to the north, somewhere between Sycamore Canyon/Sedona and the Mogollon Rim near Payson (Ross, 1973).

Whetstone Mountains (Northern Pedregosa Basin; supplemental Fig. 5)

Location and Lithofacies

This section was measured and sampled from the southeastern Whetstone Mountains north of the town of Sierra Vista, Arizona. The investigated section spans middle Pennsylvanian through middle Permian (late Wolfcampian), and samples were collected from the Horquilla Limestone and the Earp Formation (Creasy, 1967). The section ends at the base of the Colina Limestone. Within this section, the Black Prince Limestone, Horquilla Limestone, Earp Formation, and Colina Limestone comprise the lower part of the Naco Group (Ross, 1973; Armin, 1987).

The Horquilla Limestone consists of ca. 340 m of mostly thin-bedded blueish-gray fossiliferous limestone. Beds are typically massive mudstone or wackestone and often contain discontinuous banded chert. Fossils include abundant brachiopods, crinoid fragments, and small (< 5 mm) fusulinids. The Horquilla Limestone contains little siliciclastic material, and the authors collected and analyzed only one sample from a green siliciclastic siltstone within the upper portion of this unit (Supplemental Fig. 5). Siliciclastic input increases in the Earp Formation, which overlies the Horquilla Limestone via gradational and somewhat arbitrary contact at which brown, thin-bedded siltstone replaces grey limestones as the dominant facies (Gilluly, 1954; Ross and Tyrrell, 1965). The Earp formation is lithologically variable and in this section consists mostly of poorly exposed brown siltstone, thin calcic sandstone, and massive lime mudstones (Supplemental Fig. 5). The middle of this formation is marked by a distinctive and regionally exposed chert pebble conglomerate (Ross and Tyrrell, 1965; Armin, 1987). In the section sampled for this study, this interval consists of a one-meter-thick massive clast-supported chert granule conglomerate with an undulatory erosional base. This is followed by ca. 25 m of

interbedded very fine to fine-grained sandstone and horizontally laminated siliciclastic shale. Sandstones are horizontally laminated and contain current ripple cross-lamination. The upper portion of the Earp Formation consists of interbedded sandstone and limestone; sandstones are typically < 1 m thick and horizontally laminated or ripple cross-laminated. Ripple cross-strata were formed by current, and in some cases climbing current ripples. Limestone beds within this interval are typically massive, grey fossiliferous to non-fossiliferous mudstones (Supplemental Fig. 5). The upper sample collected from this section was collected from one-meter-thick quartzose sandstone with climbing current ripple cross-lamination.

Age

The ages of rocks within this section are well constrained biostratigraphically. The Black Prince limestone has been dated as Morrowan, and the Horquilla Limestone has been well dated as Atokan to Virgilian based on fusulinids (Ross and Tyrrell, 1965). The Earp Formation contains fewer fusulinids than the Horquilla Limestone, but the Red Chert Conglomerate interval that roughly bisects the Earp Formation is well dated as middle Wolfcampian (Armin, 1987). The overlying Colina Limestone is interpreted as late Wolfcampian to Leonardian (Sabins, 1957; Lyons, 1989; Armin, 1987).

Depositional Systems

The Horquilla Formation at this location is interpreted to represent deposition in an open shelf/carbonate bank environment adjacent to the deep axis of the Pedregosa Basin (Ross, 1973; Soreghan 1992). The lower Earp Formation in this location is interpreted to represent mixed carbonate/siliciclastic deposition within an inner shelf environment (Ross, 1973; Armin, 1987). The Red Chert Conglomerate that bisects the Earp Formation is interpreted as the result of a major tectonically driven regression that carved a regional erosion surface that was subsequently buried by braided fluvial deposits (Armin, 1987). Above this, thinly interbedded sandstone and shale deposits with some carbonate beds are interpreted to represent deposition within shallow- to marginal-marine environment adjacent to the deeper Pedregosa Basin to the southeast (Schreiber et al., 1990).

Central-Western Paradox Basin Transect

Location and Lithofacies

Samples were collected from three localities along a roughly northwest-southeast transect across the central central-western Paradox Basin (Burr, 2017). These three locations span distal, medial and proximal basin positions along this transect. In the distal basin position, the Honaker Trail section, we collected samples from the Paradox Formation, and the Honaker Trail Formation. From the medial basin section - Cane Creek - we collected one sample from the upper Honaker Trail Formation. In the proximal basin near Gateway, CO, we sampled the Cutler Formation Undivided. Overall, these samples span the early Desmoinesian to Wolfcampian time. The Honaker Trail section is located in the distal portion of the Paradox Basin ca. 10 km northwest from Mexican Hat, Utah. Here, the Paradox Formation consists of nested 4th and 5th order sequence stratigraphic cycles of fine grained siliciclastic and carbonate facies (Goldhammer, 1991).

Facies of the Lower Honaker Trail Formation are similar to those of the Paradox Formation with the exception that the abundance of quartzose sandstone increases, and the total thickness of

black, laminated mudstone decreases substantially (Goldhammer et al., 1991). We refer the reader to Pray and Wray (1963) and Goldhammer and others (1991) for more detailed description of the facies present at the Honaker Trail section. Samples from the Paradox and Honaker Trail Formations at both sections were collected from siliciclastic intervals within this section, either quartzose sandstones at the base of 5th order sequences or cap facies.

Cutler Formation Undivided strata (Cater, 1955; Cater and Craig, 1970) occupied a proximal basin position within the Paradox Basin, and Cutler Formation Undivided facies are in buttress unconformity with crystalline rocks of the ancient Uncompahgre Uplift ca. 10 km to the northeast (Moore et al., 2008). Samples were collected near Gateway, Colorado, ca. 60 m (JB01) and ca. 400 m (TP01) below an unconformable contact with the Triassic Moenkopi Formation placing these samples within the upper Cutler Formation (undivided) (Condon, 1997).

Age

Age determinations within this section were made based on the abundant and diverse fossil assemblages preserved within calcareous intervals (Petersen and Hite, 1969). Based on these assemblages, the Paradox Formation is interpreted as Desmoinesian to earliest Missourian, and the Honaker Trail Formation is interpreted as early Missourian to middle Virgilian (Wengerd and Matheny, 1958; Welsh, 1958; Peterson and Hite, 1969; Condon, 1997). The Cane Creek section is within uppermost Honaker Trail Formation (Hite and Lohman, 1973), interpreted as ca. Missourian in the central Paradox Basin (Baars and Stevenson, 1982).

Cutler Formation strata near Gateway, CO have not been directly dated; however, these rocks have mostly been interpreted as early Permian (Wolfcampian) in age based on regional correlations (Baars, 1962; Condon, 1997; Grazul et al., 2015).

Depositional Systems

Goldhammer and others (1991) interpreted Fifth-order sequences at this location as glacio-eustatic regressive sequences deposited on the southwestern shelf of the Paradox Basin. Quartzose sandstones at the base of idealized sequences within this section were interpreted as material transported into the distal basin shelf by eolian processes and reworked in a shoreface depozone during transgression (Goldhammer et al., 1991). See Goldhammer and others (1991) for more detailed interpretations of depositional environments.

The increased abundance of feldspatho-quartzose sandstone within the Cane Creek section (Burr, 2017) is interpreted to record material derived from erosion of the Uncompahgre uplift to the northeast (Wengerd and Matheny, 1958), and overall, this section is interpreted to represent the final stage of shallow marine deposition prior to terrestrial deposition of the overlying Cutler Formation (Condon, 1997).

Cutler Formation Undivided rocks have predominantly been interpreted as proximal subareal arid to semi-arid alluvial fan deposits shed from the Uncompahgre Uplift to the northeast (Campbell, 1980; Shultz, 1984; Mack and Rasmussen, 1984; Grazul et al., 2015). In this model, channelized, matrix- and clast-supported conglomerates near Gateway have been interpreted as debris-flow deposits filling fan-head trenches (Campbell, 1980); tabular matrix- and clast-supported conglomerates have been interpreted as unconfined debris-flows (Shultz, 1984); and sandy granule conglomerates have been interpreted as the deposits of shallow bedload stream

flows and sheetfloods (Shultz, 1984) and hyperconcentrated flood flows (Soreghan et al., 2009). Rooted siltstones are interpreted as weakly developed paleosols on overbank deposits.

Alternatively, the Cutler Formation Undivided near Gateway, CO has been interpreted to represent deposition in a Gilbert-type delta system in a cold, glacial, lacustrine system (Moore et al., 2008; Soreghan et al., 2009).

Durango to Ouray, CO (Paradox Basin)

Location and Lithofacies

Seven samples were collected from a transect across the eastern proximal Paradox basin between Durango, CO and just north of Ouray, CO. Strata in this portion of the basin are divided into the Molas Formation; the Hermosa Group, which includes the Pinkerton Trail, Paradox, and Honaker Trail Formations; the Rico Formation; and the Cutler Formation (Campbell, 1981). There is disagreement over both the Hermosa Group and the Rico Formation. Wengerd and Matheny (1958) officially upgraded the Hermosa Formation to Group rank, but both uses of the name persist (e.g. Luedke and Burbank, 1981; Nair et al., 2018). Baars (1962) recommended that the term "Rico" be completely dropped from the Paradox basin nomenclature, but the term also persists as either a transitional formation or in reference to facies between the Hermosa Group and Cutler Formation (e.g. Campbell, 1981).

The Molas Formation is deposited atop a well-developed paleokarst surface on the Mississippian Leadville Limestone (Evans and Reed, 2007; Evans and Soreghan, 2015) The Molas Formation is ca. 15-40 thick in the eastern Paradox Basin (Condon, 1992; Evans and Reed, 2007) and consists of an overall fining-upwards sequence of massive to crudely stratified matrix-supported chert breccia, clast-supported chert breccia, channelized clast-supported pebble conglomerates, and rare cross-stratified and rippled sandstone, all interbedded with massive to weakly-laminated red siltstone (Evans and Reed, 2007). Some siltstone intervals contain blocky ped structures, slickensides, root traces, and green mottling (Evans and Reed, 2007).

The Pinkerton Trail Formation consists of fossiliferous limestone containing crinoids and fusulinids interbedded with light gray siltstone (Wengerd and Strickland, 1954; Wengerd and Matheny, 1958). The formation is 26 m thick at its type section north of Durango, CO and thickens to the west into the deeper portions of the Paradox Basin (Wengerd and Matheny, 1958).

Above the Pinkerton Trail Formation in Durango area (eastern proximal Paradox Basin), the Paradox Formation is made up of channelized sandstones and conglomerates interbedded with siltstone and shale, and sparse dolomite (Wengerd and Matheny, 1958). The upper portion of the formation is dominated by black shale interbedded with limestone and dolostone. The Paradox Formation thickens from ca. 820 m north of Durango to > 1200 m in the basin center. Evaporite facies are not present in the section described here, but Paradox Formation evaporitic rocks have been documented ca. 50 to the west in the subsurface (Wengerd and Strickland, 1954).

The Honaker Trail Formation in this proximal portion of the Paradox Basin consists of nodular and fossiliferous fusulinid limestone, arkosic sandstone and rare conglomerate, and red-maroon and green siltstone intervals. Above this, the "Rico facies," considered part of the Honaker Trail Formation by most authors (Baars, 1962) and consists of fossiliferous and nodular limestone interbedded with sandstones and greenish siltstones.

The Cutler Formation (Undifferentiated) exposed in the San Juan Mountains between Durango and Ouray, CO is up to ca. 750 m thick and consists of arkosic and conglomeratic sandstones interbedded with red to brown siltstones as well as rare red-gray non-fossiliferous limestones (Baars, 1962). Individual beds vary laterally in thickness, and lenticular geometries are common within these strata (Baars, 1962). Cutler Facies in this area are substantially finer-grained than Cutler facies exposed near Gateway, CO.

Age

The age of the Molas Formation is interpreted as Morrowan to late Atokan or earliest Desmoinesian (earliest Cherokee) (Marshall, 2010) based on fauna from southwestern Colorado (Wengerd and Matheny, (1958).

The fossil assemblage within the Pinkerton Trail Formation is interpreted as Atokan through earliest Desmoinesian (Wengerd and Matheny, 1958), and the Pinkerton Trail and Molas Formations are temporally overlapping and stratigraphically interfingered.

Fossils identified from the Paradox Formation define a Desmoinesian age, and the Honaker Trail Formation is identified as Desmoinesian (Wengerd and Matheny, 1958). The Cutler Formation (Undifferentiated) is generally poorly dated (see Gateway section above). Limestone beds within Cutler facies near Ouray, CO contain Desmoinesian fossils (Baars, 1962), but the bulk of the formation is interpreted to be Wolfcampian in age, and we use this age for maps and interpretations within this study.

Depositional Systems

This sample transect is positioned within the medial (Durango, CO) to proximal (Ouray, CO) Paradox Basin. The well-developed paleo-karst surface on the Mississippian Limestone is interpreted to represent extended subaerial exposure and weathering during latest Mississippian and earliest Pennsylvanian time. The Molas Formation is interpreted to represent the gradual burial of this surface by windblown sediment, colluvium, fluvial systems (Evans and Reed, 2007). By Middle Pennsylvanian (Desmoinesian) time, shallow marine deposystems of the Hermosa Group dominated the basin (Wengerd and Matheny, 1958). No evaporitic rocks are preserved along this transect, but evaporites interpreted as representing restricted marine conditions (Baars and Stevenson, 1982) in the subsurface ca. 50 km to the west correlate with Paradox Formation rocks exposed in this transect. The Cutler Formation (Undifferentiated) is interpreted to have been deposited in a series of fluvial and alluvial fans sourced from the ancestral Uncompahgre Uplift along the northeast side of the basin (Campbell, 1980). Cutler samples collected along the Durango-Ouray transect occupy two distinct positions within this system. The Cutler Formation just north of Durango (from which we collected sample HC01) is interpreted as meandering fluvial deposits downstream of the Piedra Fan, sourced from the San Luis highland to the northeast (Campbell, 1980). The Cutler Formation north of Ouray is interpreted as having been deposited within the distal alluvial/fluvial Miguel Fan directly to the north (Campbell, 1980).

Eagle Basin Transect (supplemental Fig. 6)

Location and Lithofacies

Pennsylvanian-Permian strata within the Eagle Basin were sampled along a generally east-west transect consisting of four detailed measured sections across the basin with one outlying sample from the southeastern portion of the basin. These strata span the age range early Pennsylvanian through upper Pennsylvanian. Sampled formations include the Belden, Minturn, the Eagle Valley, the Eagle Valley Evaporite, and the Maroon.

The Belden Formation includes the oldest Eagle Basin fill and consists of cycles of black shale, dolomite, and limestone coarsening up to sandstones interbedded with black mudstones (DeVoto et al., 1986; Johnson et al., 1992).

The Minturn Formation was deposited above black shales, limestones, and fine-grained sandstones of the Belden Formation. The Minturn consists of lenticular, arkosic sandstones and conglomerates; siltstones and mudstones, and regionally continuous limestone and dolomite beds (Tweto and Lovering, 1977; Johnson, 1987). Sandstones display a range of sedimentary structures including normal and reverse graded bedding, current ripple cross stratification, and hummocky cross-stratification (Hoy and Ridgway, 2002; Lamb et al., 2008; Myrow et al., 2008). Sandstones and conglomerates within the lower portion of the Minturn are channelized, whereas those in the middle to upper portions of the formation are tabular (Hoy and Ridgway, 2002). Dark green to grey siltstones and mudstones make up a volumetrically substantial portion of the Minturn Formation (Supplemental Fig. 6; Lamb et al., 2008). Regionally extensive limestones consist of sandy, micaceous, and rarely conglomeratic micrite. These units include oolitic, foraminiferal, phylloid algal, and stromatolitic facies (Tweto and Lovering, 1977).

To the west, the Minturn (as well as the lower Maroon Formation) grade into facies of the Eagle Valley Formation and Eagle Valley Evaporite (Mallory, 1971; Schenk, 1992). A variety of names and correlations have been proposed for the Eagle Valley Formation and the Eagle Valley Evaporite (e.g. Mallory, 1971; Tweto and Lovering, 1977; Schenk, 1992), but here, we used the mapping and stratigraphic correlations of Lidke, (1992). The Eagle Valley Evaporite consists of massive gypsum deposits, gypsiferous mudstones and siltstones, chert-rich dark grey limestones, and rare sandstones and conglomerates (Mallory, 1971; Schenk, 1987). Analysis of drill core indicates the presence of anhydrite and halite in addition to the above lithologies (Mallory, 1971). Above this, the Eagle Valley Formation (sensu Mallory et al., 1987; Lidke, 2002) consist of varicolored siltstone and shale, fine grained sandstone, and gray, micritic limestone (Lidke, 2002); this formation is considered as transitional between the underlying evaporitic facies and facies of the Minturn or Maroon facies above (Tweto et al., 1978).

The Maroon Formation is defined as strata between the Jacque Mountain Limestone Member of the Minturn Formation (Supplemental Fig. 6) and the middle Permian Weber Sandstone or State Bridge Formation (Murray, 1958). The base of the Maroon Formation consists of massive to stratified siltsone, fine-grained, wave-rippled sandstones, and occasional dark grey limestone beds (Supplemental Fig. 6; Johnson, 1987). Above this, facies transition to channelized, cross-bedded sandstones and conglomeratic sandstones near the edges of the basin, and finer-grained tabular and horizontally stratified and ripple-cross stratified sandstones toward the basin center. These sandstones are commonly interbedded with mottled, massive to weakly stratified mudstones containing root traces and calcic nodules (Johnson, 1987). Tabular, >1 m thick plane-bedded and low angle cross-stratified sandstones occur throughout the formation. The upper Maroon Formation, particularly in the southeastern portion of the basin, contains abundant

massive, sandy siltstone deposits that are either tabular or weakly undulatory (Johnson, 1989; Soreghan et al., 2014).

Age

The Belden Formation is interpreted as Morrowan-Atokan by some workers (DeVoto et al., 1986; Johnson et al., 1992) and as young as Desmoinesian by others (Langenheim, 1978). Here, we interpret the age of this formation as Morrow-Atokan because the sampled interval is at the base of the formation. Age determination for the Minturn Formation relies on fossils identified from regionally extensive limestone members. Most age-diagnostic fossils have been collected from the Robinson Limestone Member, and these fossils have been interpreted as Atokan to Desmoinesian in age (Tweto and Lovering, 1977). Abundant fossils collected from the Eagle Valley Evaporite have been interpreted as late Atokan to Desmoinesian in age (Mallory, 1971). The Maroon Formation has been defined as Middle Pennsylvanian to early Permian based on well dated underlying and overlying strata (Murray, 1958; Johnson, 1987, 1989). The formation itself contains few fossils, but invertebrate fossils from thin limestone intervals near the base of the formation have been interpreted as middle Pennsylvanian (Voigt et al., 2005). Ichnofauna from the upper portion of the Formation have been interpreted as Wolfcampian, and U-Pb analyses of detrital zircons from the upper portion of the Maroon Formation yielded Wolfampian age grains (Soreghan et al., 2004, 2014). Maroon Formation samples analyzed in this study were collected from the basal portion of the Maroon Formation, and we interpret these samples as late Pennsylvanian in age.

Depositional Systems

The Belden Formation has been interpreted to represent deposition within a marine pro-delta to delta-front environment (Brill, 1944; Langenheim, 1978; Johnson et al., 1992) early in the development of the Eagle Basin system.

The Minturn Formation is interpreted to represent dominantly shallow marine conditions that were periodically overwhelmed by pulses of coarse clastic material derived from Ancestral Rocky Mountain highlands to the northeast (Tweto and Lovering, 1977). Conglomerates and channelized sandstones are interpreted to represent fan-delta and fluvial-delta deposits (Hoy and Ridgway, 2002), and thinner, tabular sandstones exhibiting normal and reverse grading, hummocky cross strata, and ripple lamination are interpreted as prodelta deposits of hyperpycnal flows influenced by oscillatory flow (Lamb et al., 2008; Myrow et al., 2008).

The Eagle Valley Evaporite and Eagle Valley Formation have been interpreted to represent deposition basin center position through evaporation of relatively deep restricted marine waters (Mallory, 1971; Johnson et al., 1992). A thick cross-bedded sandstone interval from the Eagle Valley Evaporite has been interpreted by Schenk (1987) as a eolian deposit, suggesting that the basin was subaerially exposed during at least one sea level regression.

The Maroon Formation is interpreted to represent deposition within a mixed fluvial and eolian environment (Johnson, 1987, 1989; Johnson et al., 1992) that formed in the late stages of Eagle Basin subsidence. Channelized sandstones and conglomerates and red, rooted mudstones are interpreted to represent fluvial systems draining the Front Range and Uncompahgre Uplifts to the northeast and southwest, respectively. Tabular, planar and low-angle cross-stratified sandstones are interpreted to represent periodic eolian sand-sheet deposition across much of the basin

(Johnson et al., 1992), and massive sandy siltstone intervals are interpreted as loessite deposits that accumulated in the eastern, downwind portion of the basin (Johnson 1989; Tramp et al., 2004; Soreghan et al., 2014).

Central Colorado Trough

Location and Lithofacies

Three samples spanning late Mississippian to early-middle Pennsylvanian were collected from the Central Colorado Trough northeast of Salida, CO from the Leadville, Kerber, and Sharpsdale Formations. The Kerber Formation consists of arkosic conglomerate and sandstones interbedded with red siltstones and mudstones, and dark colored, fossiliferous limestones are also common in the section (Wallace et al., 1999). Conformably overlying the Kerber Formation, the Sharpsdale Formation consists of arkosic granule and pebble conglomerates interbedded with arkosic sandstone and purple-red fine grained intervals (Wallace et al., 1999).

Age

The Kerber formation is interpreted as Morrowan to Atokan based on conodont assemblages (Musgrave, 2003), and the Sharpsdale is interpreted as Atokan based on fusulinid and conodont fossils (Musgrave, 2003).

Depositional Systems

The Kerber and Sharpsdale Formations are the oldest Pennsylvanian strata in the Central Colorado Trough, and both are interpreted to represent deposition of sediment eroded off of Ancestral Rocky Mountain highlands in shallow marine, delta, and fluvial environments (Musgrave, 2003). Based on the arkosic composition of these rocks, they are interpreted as one of the earliest records of Ancestral Rocky Mountain exhumation (Musgrave, 2003).

Manitou Springs (Denver Basin)

Location and Lithofacies

Samples were collected from the Fountain and Ingleside Formations near Manitou Springs, Colorado. This section is deposited unconformably above a paleokarst surface developed on Devonian to Mississippian Hardscrabble Limestone (Suttner et al., 1987; Keller et al., 2005) and is capped by Mesozoic rocks as young as Cretaceous (Keller et al., 2005). To the south, the section is in fault contact with the Pikes Peak Granite (Keller et al., 2005), a 1.09 Ga intrusive suite (Smith et al., 1999). The Fountain Formation is divided into the Glen Eyrie Member and Lower, Middle, and Upper Fountain Formation (Suttner et al., 1984; Sweet and Soreghan, 2010). Above this, Permian rocks have been mapped as equivalent to the Lyons Formation (Keller et al., 2005; Sweet and Soreghan, 2010), but recent work has reinterpreted these rocks as equivalent to the Ingleside Formation (Sweet et al., 2015).

At the base of the Fountain Formation, the Glen Eyrie Member consists interbedded mudstone, siltstone, limestone, sandstone, coal, conglomerate, and paleosol deposits (Suttner et al., 1984). At the southern extent of the Manitou Springs exposure, the Glen Eyrie Member (sensu Sutner et al., 1984) consists of coarse-grained deposits that progressively fine northwards. Coarse-grained southern extent of the Glen Eyrie Member as described by Suttner and others (1984) is equivalent to the Lower Fountain and part of the Middle Fountain Formation as described by

Sweet and Soreghan (2010). These rocks consist of interbedded conglomerates, sandstones, and paleosols (Sweet and Soreghan, 2010). Clast compositions of conglomerates within this member are granitic and gneissic (Sweet and Soreghan, 2010). The Lower and Middle members of the Fountain formation are separated by an angular unconformity. Clast within Middle Fountain Formation include granite, gneiss, quartzite, and fine-grained igneous lithologies. The Upper Fountain Formation consists of channelized planar- and trough cross-stratified sandstone interbedded with paleosols (Sweet and Soreghan, 2010) and conglomerate clasts are granite and gneiss (Sweet and Soreghan, 2010). Paleocurrent analysis of the Middle Fountain Formation (sensu Sweet and Soreghan, 2010) yielded paleotransport directions ranging between NW, NE, and SE (Suttner et al., 1984; Sweet and Soreghan, 2010). In contrast paleocurrent analysis of the Upper Fountain Formation yielded consistent paleotransport directions between E and SE.

The Ingleside Formation (sensu Sweet et al., 2015) is composed of feldspatho-quartzose sandstone (sensu Garzanti, 2016) with large (up to 9 m tall) planar cross-stata interbedded with massive, muddy sandstone (Sweet et al., 2015). Paleocurrent indicators based on foreset dip show dominantly SSW paleotransport (Sweet et al., 2015).

Age

The base of the Glen Eyrie Member of the Fountain Formation has been interpreted as straddling the Mississippian-Pennsylvanian Boundary (Chronic and Williams, 1978). Roughly 100 m above this, conodonts have been interpreted as Atokan in age (Suttner et al., 1984). No datable fossils are preserved in the section above this location; however, marine fossils in strata interpreted as equivalent to the Ingleside Formation (sensu Sweet et al., 2015) are interpreted as Lower Permian (Wolfcampian), and the Fountain Formation is interpreted as entirely of Pennsylvanian Age (Sweet et al., 2015). Thus, sample MS01 from the base of the Glen Eyrie Member is interpreted as Atokan in age; sample MS10 from the upper Lower Fountain Formation (sensu Sweet and Soreghan, 2010) is interpreted as Atokan; sample MS11 from the lower Middle Fountain Formation (sensu Sweet and Soreghan, 2010) is interpreted as Atokan; MS06 from the upper Middle Fountain Formation (sensu Sweet and Soreghan, 2010) is interpreted as Desmoinesian; MS05 from the lower Upper Fountain Formation and MS04 from the Upper Fountain Formation are all interpreted as Desmoinesian-Virgilian; and MS07 from the Ingleside Formation (sensu Sweet et al., 2015) is interpreted as Wolcampian.

Depositional Systems

Based on lithofacies, stratigraphic architecture, and paleocurrent analyses (where available), the Glen Eyrie Member (sensu Suttner et al., 1984) and the Lower and Middle Fountain Formation (Sensu Sweet and Soreghan, 2010) are interpreted to mixed marine and alluvial rocks deposited in an alluvial fan-delta system that spasmodically prograded northward in response to movement along the interpreted Ancestral Ute Pass Fault to the south (Suttner et al., 1984; Sweet and Soreghan, 2010). The Ancestral Ute Pass Fault is interpreted as a NW-SE oriented Pennsylvanian basement-involved structure that bounded this portion of the Fountain depositional system and shed material eroded from the Pikes Peak Batholith in the footwall into the basin; it is interpreted either as a normal fault (Suttner et al., 1984) or a thrust fault (Sweet and Soreghan, 2010). The Upper Fountain Formation is interpreted to represent the remnants of a west-southwest flowing fluvial system that post-dated uplift along the Ancestral Ute Pass Fault (Sweet and Soreghan, 2010). The Ingleside Formation (Sensu Sweet et al., 2015) is interpreted as the remnant of a large eolian system that included periodic soil formation (Sweet et al., 2015).

Keeler Canyon/Lone Pine Basin

Location and Lithofacies

Samples were collected from two subareas from the southern Inyo Mountains, near Lone Pine, CA. The northeastern area, north of the town of Lone Pine consists of the Keeler Canyon Formation and the overlying Lone Pine Formation. Five samples were collected from the Lone Pine Formation. This formation within the Owens Valley Group (Merriam and Hall, 1957; Stone and Stevens, 1987) and is subdivided, in ascending order, into Members A, B, C, and the Reward Conglomerate (Stone and Stevens, 1987). Member A consists of ca. 237 m of laminated calcareous and dolomitic mudstone; these rocks are rich in organic material and contain authigenic pyrite. Interbedded with this mudstone are sparse micritic limestone intervals. The contact with Member B is gradational, and the Member B facies are similar to those in A, but Member B contains more abundant silt and clay minerals (Stone and Stevens, 1978). Member C consists of ca. 120 m of massive quartzose siltstone interbedded with sparse quartzite pebble conglomerates (Stone et al., 2000). The Reward Conglomerate consists of ca. 200 m cross-bedded thick-bedded chert and quartzite pebble conglomerate (Stone and Stevens, 1987; Stone et al., 2000).

The other area sampled is near Conglomerate Mesa, located northeast of the town of Keeler, CA. The Pennsylvanian-Permian section in this area consists of the Keeler Canyon Formation and the informally named Sedimentary Rocks of Santa Rosa Flat, consisting of members 1-12 (Stone et al., 2009). The Keeler Canyon Formation consists calcic sandstones ranging in thickness from several centimeters to ca. 1 m interbedded with reddish calcic mudstones. Most sandstones are normally graded, contain partial Bouma sequences, and have fluted and flame and lode casts at their base. Near the base of the formation, the Keeler Canyon Formation also contains thick (several meters), calcic, matrix supported conglomerates. The Keeler Canyon sample analyzed as part of this study (KC-2) was collected from the Lower Salt Tram Member of (Stevens et al., 2001). Stratigraphically above this, the Sedimentary Rocks of Santa Rosa Flat consist of sandstone, siltstone, limestone, limestone conglomerate, and shale (Magginetti et al., 1988; Stone et al., 1989; Stone et al., 2014). Samples were collected from Members 11 and 12a, which consist of ca. 200 m of brown to grey sandstone, siltstone, and conglomerate, and interbedded maroon and light green siltstone, respectively (Stone et al., 2014).

Age

Pennsylvanian-Permian rocks within the Keeler and Lone Pine basins have been well dated biostratigraphically (eg. Stevens and Stone, 1987; Stone et al., 1987; Magginetti et al., 1988; Stevens et al., 2015a,b.). North of Lone Pine, CA, fusulinids from the Member B of the Lone Pine Formation have been interpreted as Late Wolfcampian (Stevens and Stone, 1987). Poorly preserved fusulinids collected from the base of the Reward Conglomerate Member of the Lone Pine Formation could represent either Wolfcampian of Leonardian age (Stevens and Stone, 1987).

In the Conglomerate Mesa area, Fusulinids and conodonts from the Salt Tram Member of the Keeler Canyon Formation have been interpreted as latest Pennsylvanian (Stevens et al., 2001). Fusulinids from the Sedimentary Rocks of Santa Rosa Flat have been interpreted as early Permian (Cisuralian) to Guadalupian (Stone et al., 2014), and fusulinids collected from Member

9, stratigraphically below the sampled strata indicate a Leonardian age (Magginetti et al., 1988; Stevens and Stone, 2009).

Depositional Systems

Collectively, rocks within this basin have been interpreted as forming within the Keeler, Lone Pine, and Darwin basins all of which overlap temporally or spatially. During late Mississippian time, the strata have been interpreted as marine sedimentation dominated by siliciclastic shale interpreted to have been sourced from the Antler terrane to the north (Stone et al., 2014). During Morrowan to Atokan time, a carbonate slope environment developed and was subsequently replaced beginning in Desmoinesian time by deep water sandy calcic turbidites and submarine debris flows of the Keeler Canyon Formation sourced from the edge of the shallow Bird Springs carbonate shelf to the east (Stone and Stevens, 1988; Yose and Heller, 1989; Miller and Heller, 1994; Stevens et al., 2001; Stevens et al., 2015a). This continued into early Permian (Wolfcampian) time in the northern portion of the basin, after which calcic turbidite deposition transition to deep, starved basin conditions of the Lone Pine Formation. Reward Conglomerate has been interpreted to represent deposition in shallow marine or alluvial fan environments and/or filling of the Lone Pine Basin by late Wolfcampian or Leonardian (stone and Stevens, 1987).

To the south within the Darwin basin (or sub-basin), sandy calcic turbidite deposition similar to that represented by the Keeler Canyon Formation began during early Permian and is now preserved as the Osborne Canyon Formation (Stone et al., 1987; Stevens et al., 2015b). Beginning in late Wolfcampian or early Leonardian, the Keeler and Darwin basins are interpreted to have been partitioned by an intra-basin uplift named the Conglomerate mesa Uplift that may have sedimentologically partitioned these basins (Stone and Stevens, 1988; Stevens et al., 2015a).

Additional Locations

Strata from several additional locations peripheral to the ARM system were sampled without detailed measured sections. These include the early Permian Quadrant Formation and Middle Permian Phosphoria Formation in southwest Montana (Wardlaw and Collinson, 1986; O'Neill et al., 1996), the middle Permian Rain Valley Formation in southern Arizona (Vaag, 1984), and the middle Permian Kaibab Formation in southeastern California (Stone et al., 1983).

Analytical Methods

University of California Santa Barbara

Zircon samples from the Keeler and Lone Pine basins (with the exception of KC-2) were analyzed for U and Pb isotopes and for trace element concentrations at the University of California–Santa Barbara (UCSB) Laser Ablation Split Stream (LASS) facility using a Nu Plasma HR MC-ICPMS (high resolution multi-collector–inductively coupled plasma mass spectrometer), a Nu AttoM single collector ICPMS (Nu Instruments Ltd., Wrexham, UK), and an Analyte 193 excimer ArF laser-ablation system equipped with a HeLex sample cell (Photon Machines, San Diego, USA) using a 24 mm beam. Analyses are normalized against the 91500

zircon standard as a reference material (1062 Ma; Wiedenbeck et al., 1995). Data were reduced using Iolite 2.31 software in Igor Pro 6.3. Error assessment follows Kylander-Clark et al. (2013).

University of Washington

Zircon samples Quad1 and Phos were analyzed at the University of Washington with the following methods:

Zircon crystals are extracted from 1 to 5 kg samples by traditional methods of crushing and grinding, followed by separation with a Wilfley table, heavy liquids, and a Frantz magnetic separator at the University of Washington. A split of 100 to 1000 zircon crystals, is separated to include all grain sizes, is incorporated into a 1" epoxy mount together with fragments of the Plesovice International standard zircon (Slama et al., 2008) and fragment of our internal standard zircon, GHB, coming from the Hypersolvus granite of the Golden Horn Batholith of the North Cascades (Eddy et al., 2016). The mounts are polished, imaged with a backscattered electron detector (BSE) with our in-house, JEOL 733 Superprobe microprobe to distinguish zircons from other remaining heavy minerals, and polished again prior to isotopic analysis.

U-Pb geochronology of zircons was conducted by laser ablation inductively coupled plasma mass spectrometry (LA–ICPMS) at the University of Washington. The analyses involve ablation of zircon with an Analyte G2 excimer laser (operating at a wavelength of 193 nm) using a spot diameter of 25 microns, 10 Hz pulse repetition rate and an energy fluence of 4.12 J cm-2. The ablated material is carried in helium and mixed with nitrogen into the plasma source of an iCAP RQ Quadrupole ICP-MS. Analyzed masses include 238U, 235U, 232Th, 207Pb, 206Pb, and 204Pb, with a total, combined dwell time of ~0.4 s. Each analysis consists of a 10 s integration on peaks with the laser off (for background), 38 s of acquisition with the laser firing, and a 17 s delay to purge the previous sample and prepare for the next analysis.

Data reduction is conducted with Iolite, using their Geochron Data Reduction Scheme to get U-Pb ages uncorrected for common lead (Paton et al., 2010), and the Andersen Routine of the Vizualage Data Reduction scheme (Chew et al., 2014), for U-Pb ages corrected for common lead. To ensure grains with a complex history (e.g., inheritance, Pb loss, or overgrowths, detectable amount of 204Pb) do not compromise data quality, the time-resolved pattern of 206Pb /238U is monitored closely during data reduction, and any analyses that show abnormal patterns (e.g., different fractionation from standards or jumps in value) are rejected (Gehrels et al., 2011).

Data are provided in three formats: measured isotopic ratios (already corrected for downhole fraction and instrument bias with Iolite), U-Pb ages uncorrected for common lead, and U-Pb ages corrected for common lead with the Andersen routine. For each analysis, the errors in determining 206Pb /238U result in a measurement error of ∼1–3% (at 2-sigma) in the 206Pb /238U age. The errors in measurement of 206Pb /207Pb also result in ∼1–3% uncertainty (at 2-sigma) in age for grains that are >1.0 Ga, but are substantially larger for younger grains due to low intensity of the 207Pb signal. The crossover in precision of206Pb /238U and 206Pb /207Pb ages occurs at ∼1.2 Ga. The best age for every analysis is thus determined from 206Pb /238U age for analyses with 206Pb /238U age < 1.2 Ga and from 206Pb /207Pb age for analyses with 206Pb /238U age > 1.2 Ga. 7. Analyses with >20% discordance (<80% concordance), as well

with >5% reverse discordance (<105% concordance) are included but are marked as ‘discordant’ and should be used with caution.

The accuracy of our protocol is regularly tested with our secondary standard GHB and a set of 8 international standards provided by the Arizona Laserchron facility, including FCT, Temora2, OG1, R33, TarBra, Oracle, 91500, and 9435 (contact the Laserchron for more information about ages and origin). Over one year of analysis, the average offset to the TIMS U-Pb age value for our determined ages uncorrected for common lead is less than 0.5 % for half of them (FCT, oracle, Tarbra, OG1) less than 1.5% for others (R33, 91500, Temora2, GHB); only the Paleogene 9435 standard displays a higher average offset (2.3 %), but this standard also displays high age variability when analyzed with a Multi-collector ICP-MS (Mark Pecha, Laserchron, pers. com; Gehrels et al., 2008). Ages corrected for common lead with the Andersen routine display a commonly bigger offset (~1.5%, but up to 3-5% for Proterozoic grains). We thus recommend to use the ages uncorrected for common lead.

The uncertainty resulting from the calibration correction is generally 1% (2-sigma) for both 206Pb /207Pb and 206Pb /238U ages. Uncertainties from this calibration correction are not included in the age uncertainties provided in the supplementary material and should be combined (quadratically) with the uncertainty of the age of the standard to yield an external uncertainty for each sample. This external uncertainty is reported in the auxiliary material table with our data and provides a minimum uncertainty for each set of analyses.

University of Arizona

All other zircon samples were dated at the Arizona Laserchron Center at the University of Arizona. Zircon crystals were extracted from samples by traditional methods of crushing and grinding, followed by separation with a Wilfley table, heavy liquids, and a Frantz magnetic separator. Samples were processed such that all zircons are retained in the final heavy mineral fraction. A large split of grains (generally thousands of grains) was incorporated into a 1” epoxy mount together with fragments or loose grains of Sri Lanka, FC-1, and R33 zircon crystals that are used as primary standards. The mounts were sanded down to a depth of ~20 microns, polished, imaged, and cleaned prior to isotopic analysis.

U-Pb geochronology of zircons was conducted by laser ablation inductively coupled plasma mass spectrometry (LA-ICPMS) at the Arizona LaserChron Center (Gehrels et al., 2006, 2008; Gehrels and Pecha, 2014). The analyses involve ablation of zircon with a Photon Machines Analyte G2 excimer laser equipped with HelEx ablation cell using a spot diameter of 20 microns. The ablated material is carried in helium into the plasma source of an Element2 HR ICPMS, which sequences rapidly through U, Th, and Pb isotopes. Signal intensities are measured with an SEM that operates in pulse counting mode for signals less than 50K cps, in both pulse-counting and analog mode for signals between 50K and 5M cps, and in analog mode above 5M cps. The calibration between pulse-counting and analog signals is determined line-by-line for signals between 50K and 5M cps, and is applied to >5M cps signals. Four intensities are determined and averaged for each isotope, with dwell times of 0.0052 sec for 202, 0.0075 sec for 204, 0.0202 sec for 206, 0.0284 sec for 207, 0.0026 sec for 208, 0.0026 sec for 232, and 0.0104 sec for 238.

With the laser set an energy density of ~5 J/cm2, a repetition rate of 8 hz, and an ablation time of 10 seconds, ablation pits are ~12 microns in depth. Sensitivity with these settings is approximately ~5,000 cps/ppm. Each analysis consists of 5 sec on peaks with the laser off (for backgrounds), 10 sec with the laser firing (for peak intensities), and a 20 second delay to purge the previous sample and save files.

Prior to analysis, grains are imaged to provide a guide for locating analysis pits in optimal locations, and to assist in interpreting results. Images are made with a Hitachi 3400N SEM and a Gatan CL2 detector system (www.geoarizonasem.org). In general, BSE images are made for detrital mounts and CL images are made for igneous mounts.

Following analysis, data reduction is performed with an in-house Python decoding routine and an Excel spreadsheet (E2agecalc) that:

1. Decodes .dat files from the Thermo software such individual intensities for measurement are available (routine written by John Hartman, University of Arizona)
2. Imports intensities and a sample name for each analysis
3. Calculates average intensities for each isotope (based on the sum of all counts while the laser is firing)
4. Subtracts 204Hg from the 204 signal to yield 204Pb intensity (using natural 202Hg/204Hg of 4.3). This Hg correction is not significant for most analyses because our Hg backgrounds are low (generally ~150 cps at mass 204).
5. Performs a common Pb correction based on the measured 206Pb/204Pb and the assumed composition of common Pb based on Stacey and Kramers (1975)
6. Calculates measured 206/238, 206/207, and 208/232 ratios
7. Compares measured and known ratios for the three standards to determine fractionation factors for 206/238, 206/207, and 208/232. These correction factors are generally <5% for 206/238, <2% for 206/207, and <20% for 208/232.
8. Determines an overdispersion factor if the standard analyses show greater dispersion than expected from measurement uncertainties
9. Uses a sliding-window average to apply fractionation factors to unknowns (generally averaging 8 standard analyses)
10. Calculates fractionation-corrected 206/238, 206/207, and 208/232 ratios and ages for unknowns
11. Propagates measurement uncertainties for 206/238 and 208/232 that are based on the scatter about a regression of measured values. Uncertainties for 206/207 and 206/204 are based on the standard deviation of measured values since these ratios generally do not change during an analysis. The sum of this uncertainty and any overdispersion factor is reported as the internal (or measurement) uncertainty for each analysis. These uncertainties are reported at the 1-sigma level.
12. Calculates the down-hole slope of 206/238 to highlight analyses in which 206/238 is compromised due to heterogeneity in age (e.g., crossing an age boundary) or intersection of a fracture or inclusion.
13. Calculates concentrations of U and Th for unknowns based on the measured intensity and known concentrations of FC-1.
14. Calculates the external (systematic) uncertainties for 206/238, 206/207, and 208/232, which

include contributions from (a) the scatter of standard analyses, (b) uncertainties in the ages of the standards, (c) uncertainties in the composition of common Pb, and (4) uncertainties in the decay constants for 235U and 238U.
15. Determines a “Best Age” for each analysis, which is generally the 206/238 age for <900 Ma ages and the 206/207 age for >900 Ma ages.
16. Provides preliminary filters that highlight analyses with >20% discordance, >5% reverse discordance, or >10% internal (measurement) uncertainty.
17. Corrects 206/238U ages for U-Th disequilibrium. This has a significant impact only on very young (~<2 Ma) ages.
18. Calculates the radiation dosage that the analyzed portion of each zircon has experienced, assuming a value of 2.3 for the Th/U of the magma. This is plotted against 206/238 age to help identify Pb loss.

References Cited

Armin, R. A., 1987, Sedimentology and tectonic significance of Wolfcampian (Lower Permian) conglomerates in the Pedregosa basin: Southeastern Arizona, southwestern New Mexico, and northern Mexico: Geological Society of America Bulletin, v. 99, no. 1, p. 42-65.

Baars, D., and Stevenson, G., 1982, Subtle stratigraphic traps in Paleozoic rocks of Paradox basin, American Association of Petroleum Geologists, AAPG Special Volumes: The Deliberate Search for the Subtle Trap.

Baars, D. L., 1962, Permian system of Colorado plateau: AAPG Bulletin, v. 46, no. 2, p. 149-218.

Blakey, R. C., 1990, Stratigraphy and geologic history of Pennsylvanian and Permian rocks, Mogollon Rim region, central Arizona and vicinity: Geological Society of America Bulletin, v. 102, no. 9, p. 1189-1217.

Blakey, R. C., and Knepp, R., 1989, Pennsylvanian and Permian geology of Arizona, in Jenney, J. P., and Reynolds, S. J., eds., Geologic evolution of Arizona: Arizona Geological Society Digest, Volume 17, p. 313-347.

Blakey, R. C., and Middleton, L. T., 1983, Permian shoreline eolian complex in central Arizona: dune changes in response to cyclic sealevel changes, Developments in Sedimentology, Volume 38, Elsevier, p. 551-581.

Blakey, R. C., Peterson, F., and Kocurek, G., 1988, Synthesis of late Paleozoic and Mesozoic eolian deposits of the Western Interior of the United States: Sedimentary Geology, v. 56, no. 1-4, p. 3-125.

Blazey, E. B., 1971, Fossil flora of the Mogollon Rim [Ph.D. thesis]: Arizona State University, 169 p.

Brew, D., 1965, The Naco Formation (Pennsylvanian) in central Arizona [PhD thesis]: Cornell University, 201 p.

Brew, D. C., and Beus, S. S., 1976, A middle Pennsylvanian fauna from the Naco Formation near Kohl Ranch, central Arizona: Journal of Paleontology, p. 888-906.

Brill Jr, K. G., 1944, Late Paleozoic stratigraphy, west-central and northwestern Colorado: Bulletin of the Geological Society of America, v. 55, no. 5, p. 621-655.

Burr, G. L., 2017, Provenance of Desmoinesian to Early Wolfcampian Strata in the Eagle and Paradox Basins, Ancestral Rocky Mountains [M.S.: Northern Arizona University.

Campbell, J. A., Lower Permian depositional systems and Wolfcampian paleogeography, Uncompahgre basin, eastern Utah and southwestern Colorado, in Proceedings Paleozoic Paleogeography of the West-Central United States: Rocky Mountain Symposium 11980, Rocky Mountain Section (SEPM), p. 327-340.

Campbell, J. A., 1981, Summary of Paleozoic stratigraphy and history of western Colorado and eastern Utah, in Epis, R. C., and Callender, J. F., eds., Western Slope (Western Colorado), Volume New Mexico Geological Society 32nd Annual Fall Field Conference Guidebook, p. 81-87.

Cater, F. W., and Craig, L. C., 1970, Geology of the salt anticline region in southwestern Colorado.

Cater Jr, F. W., 1955, The salt anticlines of southwestern Colorado and southeastern Utah, Four Corners Geological Society, Geology of Parts of Paradox, Black Mesa and San Juan Basins, Four Corners Field Conference.

Chew, D., Petrus, J., and Kamber, B., 2014, U–Pb LA–ICPMS dating using accessory mineral standards with variable common Pb: Chemical Geology, v. 363, p. 185-199.

Chronic, J., and Williams, C. A., 1978, The Glen Eyrie Formation (Carboniferous) near Colorado Springs, Energy Resources of the Denver Basin, Rocky Mountain Association of Geologists - 1978 Symposium, p. 199-206.

Condon, S. M., 1997, Geology of the Pennsylvanian and Permian cutler group and Permian Kaibab limestone in the Paradox Basin, southeastern Utah and southwestern Colorado, US Government Printing Office, v. 2000.

Creasy, S., 1967, Geologic map of the Benson quadrangle, Cochise and Pima counties, Arizona: USGS.

DeVoto, R., Bartleson, B., Schenk, C., and Waechter, N., 1986, Late Paleozoic stratigraphy and syndepositional tectonism, northwestern Colorado: New interpretations of northwest Colorado geology: Denver, Colorado, Rocky Mountain Association of Geologists, p. 37-49.

Dunbar, C. O., and Condra, G. E., 1927, The Fusulinidae of the Pennsylvanian system in Nebraska: Bulletin of the Nebraska Geological Survey, series 2, v. 2, p. 1-135.

Eddy, M. P., Bowring, S. A., Miller, R. B., and Tepper, J. H., 2016, Rapid assembly and crystallization of a fossil large-volume silicic magma chamber: Geology, v. 44, no. 4, p. 331-334.

Evans, J. E., and Reed, J. M., 2007, Integrated loessite-paleokarst depositional system, early Pennsylvanian Molas formation, Paradox Basin, southwestern Colorado, USA: Sedimentary Geology, v. 195, no. 3-4, p. 161-181.

Evans, J. E., and Soreghan, M., 2015, Long-distance sediment transport and episodic resedimentation of Pennsylvanian dust (eolian silt) in cave passages of the Mississippian Leadville Limestone, southwestern Colorado, USA, in Feinberg, J., Gao, Y., and Alexander, E. C., Jr., eds., Caves and Karst Across Time, Volume Geological Society of America Special Paper 516, p. 1-22.

Garzanti, E., 2016, From static to dynamic provenance analysis—Sedimentary petrology upgraded: Sedimentary Geology, v. 336, p. 3-13.

Gehrels, G., 2011, Detrital zircon U-Pb geochronology: Current methods and new opportunities, in Busby, C., and Azor, A., eds., Tectonics of sedimentary basins: Recent advances, Blackwell Publishing Ltd, p. 45-62.

Gehrels, G., and Pecha, M., 2014, Detrital zircon U-Pb geochronology and Hf isotope geochemistry of Paleozoic and Triassic passive margin strata of western North America: Geosphere, v. 10, no. 1, p. 49-65.

Gehrels, G., Valencia, V., and Pullen, A., 2006, Detrital zircon geochronology by laser-ablation multicollector ICPMS at the Arizona LaserChron Center: The Paleontological Society Papers, v. 12, p. 67-76.

Gehrels, G. E., Valencia, V. A., and Ruiz, J., 2008, Enhanced precision, accuracy, efficiency, and spatial resolution of U-Pb ages by laser ablation–multicollector–inductively coupled plasma–mass spectrometry: Geochemistry, Geophysics, Geosystems, v. 9, no. 3.

Gilluly, J., Cooper, J. R., and Williams, J. S., 1954, Late Paleozoic stratigraphy of central Cochise county, Arizona: United States Geological Survey, 2330-7102.

Goldhammer, R., Oswald, E., and Dunn, P., 1991, Hierarchy of stratigraphic forcing: Example from Middle Pennsylvanian shelf carbonates of the Paradox Basin: Sedimentary Modeling: Computer Simulations and Methods for Improved Parameter Definition: Kansas Geological Survey, Bulletin, v. 233, p. 361-413.

Grazul, K. R., Huntoon, J. E., and O'Keefe, J. M., 2015, Stratigraphy and fossil plants from the Cutler Formation (Late Paleozoic) and their paleoclimatic implications, eastern Paradox Basin, Colorado: Geology of the Intermountain West, v. 2, p. 9-27.

Hite, R. J., and Lohman, S. W., 1973, Geologic appraisal of Paradox basin salt deposits for water emplacement: US Geological Survey.

Hoy, R. G., and Ridgway, K. D., 2002, Syndepositional thrust-related deformation and sedimentation in an Ancestral Rocky Mountains basin, Central Colorado trough, Colorado, USA: Geological Society of America Bulletin, v. 114, no. 7, p. 804-828.

Huddle, J. W., and Dobrovolny, E., 1945, Late Paleozoic stratigraphy and oil and gas possibilities of central and northeastern Arizona: United States Geological Survey.

Hughes, P. W., 1952, Stratigraphy of Supai Formation, Chino Valley area, Yavapai County, Arizona: AAPG Bulletin, v. 36, no. 4, p. 635-657.

Johnson, S. Y., 1987, Stratigraphic and sedimentologic studies of late Paleozoic strata in the Eagle basin and northern Aspen sub-basin, northwest Colorado: US Geological Survey, 2331-1258.

-, 1989, Significance of loessite in the Maroon Formation (middle Pennsylvanian to lower Permian), Eagle basin, Northwest Colorado: Journal of Sedimentary Research, v. 59, no. 5, p. 782-791.

Johnson, S. Y., Chan, M. A., and Konopka, E., 1992, Pennsylvanian and Early Permian paleogeography of the Uinta-Piceance basin region, northwestern Colorado and northeastern Utah, US Department of the Interior, US Geological Survey, U.S. Geological Survey Bulletin, v. 1787.

Kauffman, A., and Roth, R., 1966, Upper Pennsylvanian and Lower Permian fusulinids from north-central Texas, Cushman Foundation for Foraminiferal Research, Special Publication, 49 p.:

Keller, J., Siddoway, C., Morgan, M., Route, E., Grizzell, M., Sacerdoti, R., and Stevenson, A., 2005, Geologic map of the Manitou Springs 7.5-minute quadrangle.

Kenny, R., and Neet, K., 1993, Upper Pennsylvanian-Permian (Naco Group) paleosols (north-central Arizona): field and isotopic evidence: Geoderma, v. 58, no. 3-4, p. 131-148.

Kocurek, G., and Day, M., 2018, What is preserved in the aeolian rock record? A Jurassic Entrada Sandstone case study at the Utah–Arizona border: Sedimentology, v. 65, no. 4, p. 1301-1321.

Kocurek, G., and Fielder, G., 1982, Adhesion structures: Journal of Sedimentary Research, v. 52, no. 4, p. 1229-1241.

Kylander-Clark, A. R., Hacker, B. R., and Cottle, J. M., 2013, Laser-ablation split-stream ICP petrochronology: Chemical Geology, v. 345, p. 99-112.

Lamb, M., Myrow, P., Lukens, C., Houck, K., and Strauss, J., 2008, Deposits from wave-influenced turbidity currents: Pennsylvanian Minturn Formation, Colorado, USA: Journal of Sedimentary Research, v. 78, no. 7, p. 480-498.

Lane, C. L., 1979, Regional Correlation of the Esplanade Sandstone, West-Central Arizona, Permianland: Four Corners Geological Society Guidebook, p. 81-85.

Langenheim Jr, R., 1978, Belden Shale Sections at Fossil Ridge and Mosca, Gunnison County, Colorado: The Wyoming Geological Association Earth Science Bulletin, v. 11, no. 4, p. 15-22.

Lidke, D. J., 2002, Geologic map of the Eagle quadrangle, Eagle County, Colorado.

Luedke, R. G., and Burbank, W. S., 1981, Geologic map of the Uncompahgre (Ouray) mining district, southwestern Colorado: United States Geological Survey.

Lyons, T. W., 1989, Stratigraphy and depositional environment of the Colina limestone (lower Permian), southeastern Arizona [MS: University of Arizona.

Mack, G. H., and Rasmussen, K. A., 1984, Alluvial-fan sedimentation of the Cutler Formation (Permo-Pennsylvanian) near Gateway, Colorado: Geological Society of America Bulletin, v. 95, no. 1, p. 109-116.

Magginetti, R. T., Stevens, C. H., and Stone, P., 1988, Early Permian fusulinids from the Owens Valley Group, east-central California, Geological Society of America Special Paper No. 217.

Mallory, W., 1971, The Eagle Valley Evaporite, northwest Colorado-a regional synthesis U.S. Geological Survey Bulletin, v. 1311-E.

Marshall, T. R., 2010, Conodont-based correlation of major cyclothems in lower Cherokee Group (lower Desmoinesian, Middle Pennsylvanian), Oklahoma to Iowa [Ph.D.: University of Iowa.

McKee, E. D., 1982, The Supai Group of Grand Canyon, US Department of the Interior, Geological Survey.

McKee, E. D., and Gutschick, R. C., 1969, History of the Redwall Limestone of northern Arizona, Geological Society of America.

McQuarrie, N., and Oskin, M., 2010, Palinspastic restoration of NAVDat and implications for the origin of magmatism in southwestern North America: Journal of Geophysical Research: Solid Earth, v. 115, no. B10.

McQuarrie, N., and Wernicke, B. P., 2005, An animated tectonic reconstruction of southwestern North America since 36 Ma: Geosphere, v. 1, no. 3, p. 147-172.

Merriam, C. W., and Hall, W. E., 1957, Pennsylvanian and Permian rocks of the southern Inyo Mountains, California: US Geological Survey Bulletin, v. 1061-A, p. 13.

Miller, F., 1970, Geologic map of the Quartzite quadrangle, Yuma County, Arizona: United States Geological Survey.

Miller, F., and McKee, E., 1971, Thrust and strike-slip faulting in the Plomosa Mountains, southwestern Arizona: Geological Society of America Bulletin, v. 82, no. 3, p. 717-722.

Miller, R. P., and Heller, P. L., 1994, Depositional framework and controls on mixed carbonate-siliciclastic gravity flows: Pennsylvanian-Permian shelf to basin transect, south-western Great Basin, USA: Sedimentology, v. 41, no. 1, p. 1-20.

Moore, K. D., Soreghan, G. S., and Sweet, D. E., 2008, Stratigraphic and structural relations in the proximal Cutler Formation of the Paradox Basin: Implications for timing of movement on the Uncompahgre front: The Mountain Geologist, v. 45, no. 2, p. 49-68.

Murray, H. F., 1958, Pennsylvanian stratigraphy of the Maroon trough, Symposium on Pennsylvanian Rocks of Colorado and Adjacent Areas, Rocky Mountain Association of Geologists, p. 47-58.

Musgrave, B. E., 2003, Lower Pennsylvanian stratigraphy of the Central Colorado Trough [M.S.: Texas Tech University.

Myers, D. A., 1958, Stratigraphic distribution of some fusulinids from the Thrifty Formation, Upper Pennsylvanian, central Texas: Journal of Paleontology, p. 677-681.

Myrow, P., Lukens, C., Lamb, M., Houck, K., and Strauss, J., 2008, Dynamics of a transgressive prodeltaic system: Implications for geography and climate within a Pennsylvanian intracratonic basin, Colorado, USA: Journal of Sedimentary Research, v. 78, no. 8, p. 512-528.

Nair, K., Holm-Denoma, C., Singleton, J., and Egenhoff, S., 2018, Detrital Zircon Geochronology of Pennsylvanian-Permian Strata in Colorado: Evidence for Appalachian-Derived Sediment and Implications for the Timing of Ancestral Rocky Mountains Uplift: The Mountain Geologist, v. 55, no. 3, p. 119-140.

O'Neill, J., Klepper, M., Smedes, H., Hanneman, D., Fraser, G., and Mehnert, H., 1996, Geologic map and cross sections of the central and southern Highland Mountains, southwestern Montana: U.S. Geological Survey, scale 1:50,000.

Paton, C., Woodhead, J. D., Hellstrom, J. C., Hergt, J. M., Greig, A., and Maas, R., 2010, Improved laser ablation U-Pb zircon geochronology through robust downhole fractionation correction: Geochemistry, Geophysics, Geosystems, v. 11, no. 3.

Peirce, H., Jones, N., and Rogers, R., 1977, A survey of uranium favorability of Paleozoic rocks in the Mogollon Rim and Slope region, east-central Arizona: Tucson: Arizona Bureau of Geological and Mineral Technology Circular, v. 19, p. 60.

Peirce, H. W., 1979, The Mississippian and Pennsylvanian (Carboniferous) Systems in the United States-Arizona.

Peirce, H. W., 1989, Correlation problems of Pennsylvanian-Permian strata of the Colorado Plateau of Arizona: Geologic evolution of Arizona. Arizona Geological Society, Tucson, p. 349-368.

Peterson, J. A., and Hite, R. J., 1969, Pennsylvanian evaporite-carbonate cycles and their relation to petroleum occurrence, southern Rocky Mountains: AAPG bulletin, v. 53, no. 4, p. 884-908.

Pray, L. C., and Wray, J. L., 1963, Porous algal facies (Pennsylvanian) Honaker Trail, San Juan Canyon, Utah, Four Corners Geological Society, Shelf Carbonates of the Paradox Basin, Fourth Field Conference, 1963.

Richard, S. M., 1992, Detailed geologic map of the upper Apache Wash area, central southern Plomosa Mountains, west-central Arizona: Arizona Geological Survey.

Richard, S. M., 1993, Palinspastic reconstruction of southeastern California and southwestern Arizona for the middle Miocene: Tectonics, v. 12, no. 4, p. 830-854.

Richard, S. M., Spencer, J. E., Tosdal, R. M., and Stone, P., 1993, Geologic map of the southern Plomosa Mountains, La Paz county, Arizona.

Ross, C. A., 1973, Pennsylvanian and Early Permian depositional history, southeastern Arizona: AAPG Bulletin, v. 57, no. 5, p. 887-912.

Ross, C. A., and Tyrrell Jr, W. W., 1965, Pennsylvanian and Permian fusulinids from the Whetstone Mountains, southeast Arizona: Journal of Paleontology, p. 615-635.

Sabins Jr, F. F., 1957, Stratigraphic relations in Chiricahua and Dos Cabezas Mountains, Arizona: AAPG Bulletin, v. 41, no. 3, p. 466-510.

Sabins Jr, F. F., and Ross, C. A., 1963, Late Pennsylvanian-early Permian fusulinids from southeast Arizona: Journal of Paleontology, p. 323-365.

Schenk, C., 1992, Stratigraphic correlations between the Eagle Valley Evaporite and Minturn Formation Eagle Basin, northwest Colorado: : U.S. Geological Survey Bulletin, v. 1787.

Schenk, C. J., 1987, Sedimentology of an eolian sandstone from the middle Pennsylvanian Eagle Valley evaporite, Eagle basin, northwest Colorado: U.S. Geological Survey Bulletin, v. 1787-B, p. 19-28.

Schreiber Jr, J., Armin, R., Armstrong, A., Connolly, W., Lyons, T., Stanton Jr, R., and Wrucke, C., 1990, Upper Paleozoic stratigraphy of the Whetstone Mountains, Cochise and Pima counties, Arizona: Geologic excursions through the Sonoran Desert region, Arizona and Sonora: Arizona Geological Survey Special Paper, v. 7, p. 104-113.

Shultz, A. W., 1984, Subaerial debris-flow deposition in the upper Paleozoic Cutler Formation, western Colorado: Journal of Sedimentary Research, v. 54, no. 3, p. 759-772.

Sláma, J., Košler, J., Condon, D. J., Crowley, J. L., Gerdes, A., Hanchar, J. M., Horstwood, M. S., Morris, G. A., Nasdala, L., and Norberg, N., 2008, Plešovice zircon—a new natural reference material for U–Pb and Hf isotopic microanalysis: Chemical Geology, v. 249, no. 1-2, p. 1-35.

Smith, D. R., Noblett, J., Wobus, R. A., Unruh, D., Douglass, J., Beane, R., Davis, C., Goldman, S., Kay, G., and Gustavson, B., 1999, Petrology and geochemistry of late-stage intrusions of the A-type, mid-Proterozoic Pikes Peak batholith (Central Colorado, USA): implications for petrogenetic models: Precambrian Research, v. 98, no. 3-4, p. 271-305.

Soreghan, G. S., 1992, Sedimentology and process stratigraphy of the upper Pennsylvanian, Pedregosa (Arizona) and Orogrande (New Mexico) basins [PhD: University of Arizona.

Soreghan, G. S., Hamilton, M., Fanning, C., Soreghan, M., Link, P., Tramp, K., and Elmore, R., The age of the Maroon loessite (Colorado), and implications for resolving high-frequency climate change in the late Paleozoic icehouse, in Proceedings Geological Society of America Abstracts with Programs2004, Volume 36, p. 66.

Soreghan, G. S., Soreghan, M. J., Sweet, D. E., and Moore, K. D., 2009, Hot fan or cold outwash? Hypothesized proglacial deposition in the upper Paleozoic Cutler Formation, western tropical Pangea: Journal of Sedimentary Research, v. 79, no. 7, p. 495-522.

Soreghan, M. J., Heavens, N., Soreghan, G. S., Link, P. K., and Hamilton, M. A., 2014, Abrupt and high-magnitude changes in atmospheric circulation recorded in the Permian Maroon Formation, tropical Pangaea: Geological Society of America Bulletin, v. 126, no. 3-4, p. 569-584.

Spencer, J. E., Youberg, A., Love , D., Pearthree , P. A., Steinke, T. R., and Reynolds, S. J., 2015, Geologic map of the Bouse and Ibex Peak 7 ½ ’ Quadrangles, La Paz County, Arizona.

Stacey, J. t., and Kramers, J., 1975, Approximation of terrestrial lead isotope evolution by a two-stage model: Earth and planetary science letters, v. 26, no. 2, p. 207-221.

Stevens, C., Stone, P., and Ritter, S., 2001, Conodont and fusulinid biostratigraphy and history of the Pennsylvanian to lower Permian Keeler Basin, east-central California: Brigham Young University Geology Studies, v. 46, p. 99-142.

Stevens, C. H., Stone, P., and Magginetti, R. T., 2015a, Regional implications of new chronostratigraphic and paleogeographic data from the Early Permian Darwin Basin, east-central California: Stratigraphy, v. 12, no. 2, p. 149-166.

Stevens, C. H., Stone, P., Magginetti, R. T., and Ritter, S. M., 2015b, Stratigraphy and paleogeographic significance of a Late Pennsylvanian to Early Permian channeled slope sequence in the Darwin Basin, southern Darwin Hills, east-central California: Stratigraphy, v. 12, no. 2, p. 185-196.

Stone, P., Dunne, G., Stevens, C., and Gulliver, R., 1989, Geologic map of Paleozoic and Mesozoic rocks in parts of the Darwin and adjacent quadrangles, Inyo County, California: USGS.

Stone, P., Dunne, G. C., Moore, J. G., and Smith, G. I., 2000, Geologic Map of the Lone Pine 15' Quadrangle, Inyo County, California: US Geological Survey.

Stone, P., Howard, K. A., and Hamilton, W., 1983, Correlation of metamorphosed Paleozoic strata of the southeastern Mojave Desert region, California and Arizona: Geological Society of America Bulletin, v. 94, no. 10, p. 1135-1147.

Stone, P., and Stevens, C. H., 1987, Stratigraphy of the Owens Valley Group (Permian), Southern Inyo Mountains, California: US Geological Survey Bulletin, v. 1692, p. 1-19.

Stone, P., and Stevens, C. H., 1988, Pennsylvanian and Early Permian paleogeography of east-central California: Implications for the shape of the continental margin and the timing of continental truncation: Geology, v. 16, no. 4, p. 330-333.

Stone, P., Stevens, C. H., and Magginetti, R. T., 1987, Pennsylvanian and Permian stratigraphy of the northern Argus Range-Darwin Canyon area, California: U.S. Geological Survey Bulletin, v. 1691.

Stone, P., Swanson, B. J., Stevens, C. H., Dunne, G., and Priest, S. S., 2014, Geologic Map of the Southern Inyo Mountains and Vicinity, Inyo County, California: US Geologlical Survey.

Stone, P., Swanson, B. J., Stevens, C. H., Dunne, G. C., and Priest, S. S., 2009, Geologic map of the southern Inyo Mountains and vicinity, Inyo County, California: US Geological Survey.

Stoyanow, A., 1942, Paleozoic paleogeography of Arizona: Bulletin of the Geological Society of America, v. 53, no. 9, p. 1255-1282.

Suttner, L. J., Langford, R. P., and O'Connell, A. F., 1984, New interpretation of the stratigraphic relationship between the Fountain Formation and its Glen Eyrie Member, in Suttner, L. J., Langford, R. P., and Schulz, A. W., eds., Sedimentology of the Fountain Fan-delta Complex near Manitou Springs and Canon City, Colorado, Volume Society of Economic Paleontologists and Mineralogists 1984 Spring Field Conference Guidebook, p. 31-61.

Sweet, D. E., Carsrud, C. R., and Watters, A. J., 2015, Proposing an entirely Pennsylvanian age for the Fountain Formation through new lithostratigraphic correlation along the Front Range: The Mountain Geologist, v. 52, p. 43-70.

Sweet, D. E., and Soreghan, G. S., 2010, Late Paleozoic tectonics and paleogeography of the ancestral Front Range: Structural, stratigraphic, and sedimentologic evidence from the Fountain Formation (Manitou Springs, Colorado): Bulletin, v. 122, no. 3-4, p. 575-594.

Tramp, K. L., Soreghan, G., and Elmore, R. D., 2004, Paleoclimatic inferences from paleopedology and magnetism of the Permian Maroon Formation loessite, Colorado, USA: Geological Society of America Bulletin, v. 116, no. 5-6, p. 671-686.

Tweto, O., and Lovering, T. S., 1977, Geology of the Minturn 15-minute quadrangle, Eagle and Summit counties, Colorado, US Government Printing Office, U.S. Geological Survey Professional Paper.

Tweto, O., Moench, R. H., and Reed Jr, J., 1978, Geologic map of the Leadville 1 degree by 2 degrees Quadrangle, northwestern Colorado: U.S. Geological Survey.

Vaag, M. K., 1984, Stratigraphy of the Permian Rainvalley Formation, southeastern Arizona [M.S.: University of Arizona, 135 p.

Voigt, S., Small, B., and Sanders, F., 2005, A diverse terrestrial ichnofauna from the Maroon Formation (Pennsylvanian-Permian), Colorado: Biostratigraphic and paleoecological significance: New Mexico Museum of Natural History and Science Bulletin, v. 30, p. 342-351.

Wallace, C., Cappa, J. A., and Lawson, A. D., 1999, Geologic map of the Gribbles Park quadrangle Park and Fremont Counties, Colorado, Colorado Geological Survey.

Wardlaw, B. R., and Collinson, J. W., 1986, Paleontology and deposition of the Phosphoria Formation: Rocky Mountain Geology, v. 24, no. 2, p. 107-142.

Weisman, M. K., 1986, Geology of the Pine and northern Buckhead Mesa quadrangles, central Arizona [M.S. thesis]: Northern Arizona University, 126 p.

Welsh, J. E., 1958, Faunizones of the Pennsylvanian and Permian rocks in the Paradox basin.

Wengerd, S. A., and Matheny, M. L., 1958, Pennsylvanian system of Four Corners region: AAPG Bulletin, v. 42, no. 9, p. 2048-2106.

Wengerd, S. A., and Strickland, J. W., 1954, Pennsylvanian stratigraphy of Paradox salt basin, Four Corners region, Colorado and Utah: AAPG Bulletin, v. 38, no. 10, p. 2157-2199.

White, D., 1928, Flora of the Hermit Shale, Grand Canyon, Arizona, Carnegie Institution of Washington, 221 p.:

Wiedenbeck, M., Alle, P., Corfu, F., Griffin, W., Meier, M., Oberli, F. v., Quadt, A. v., Roddick, J., and Spiegel, W., 1995, Three natural zircon standards for U-Th-Pb, Lu-Hf, trace element and REE analyses: Geostandards newsletter, v. 19, no. 1, p. 1-23.

Winters, S. S., 1963, Supai Formation (Permian) of eastern Arizona, Geological Society of America Memoir, 99 p.:

Wrucke, C. T., Bromfield, C. S., Simons, F. S., Greene, R. C., Houser, B. B., Miller, R. J., and Gray, F., 2004, Geologic map of the San Carlos Indian Reservation, Arizona: US Geological Survey.

Yose, L. A., and Heller, P. L., 1989, Sea-level control of mixed-carbonate-siliciclastic, gravity-flow deposition: Lower part of the Keeler Canyon Formation (Pennsylvanian), southeastern California: Geological Society of America Bulletin, v. 101, no. 3, p. 427-439.

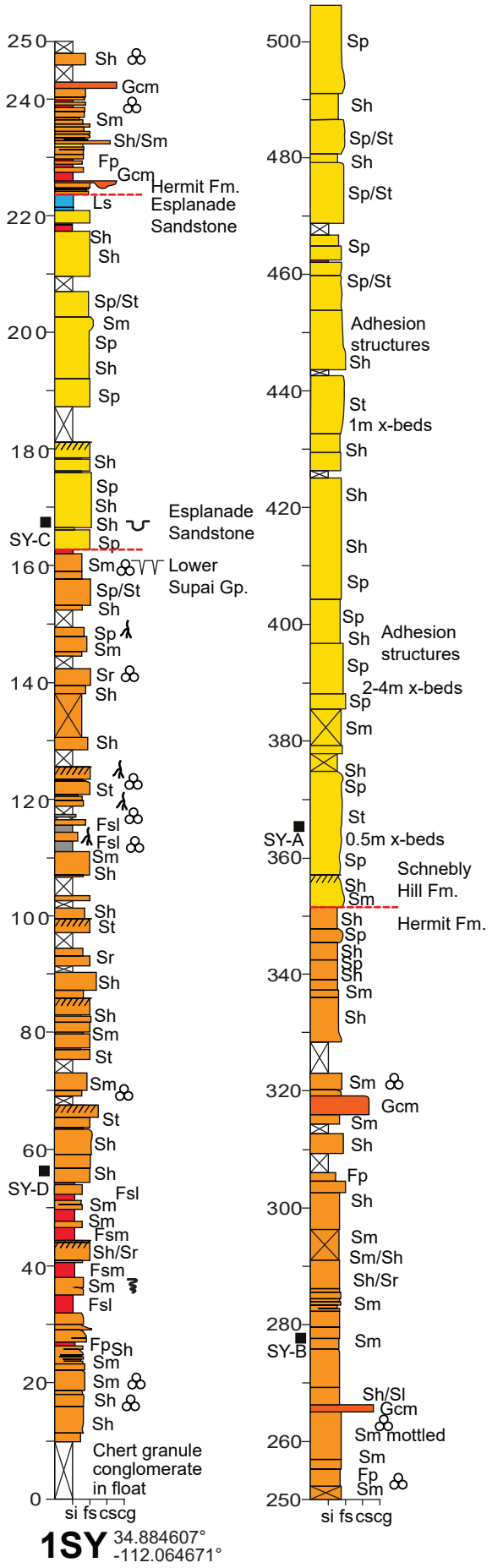

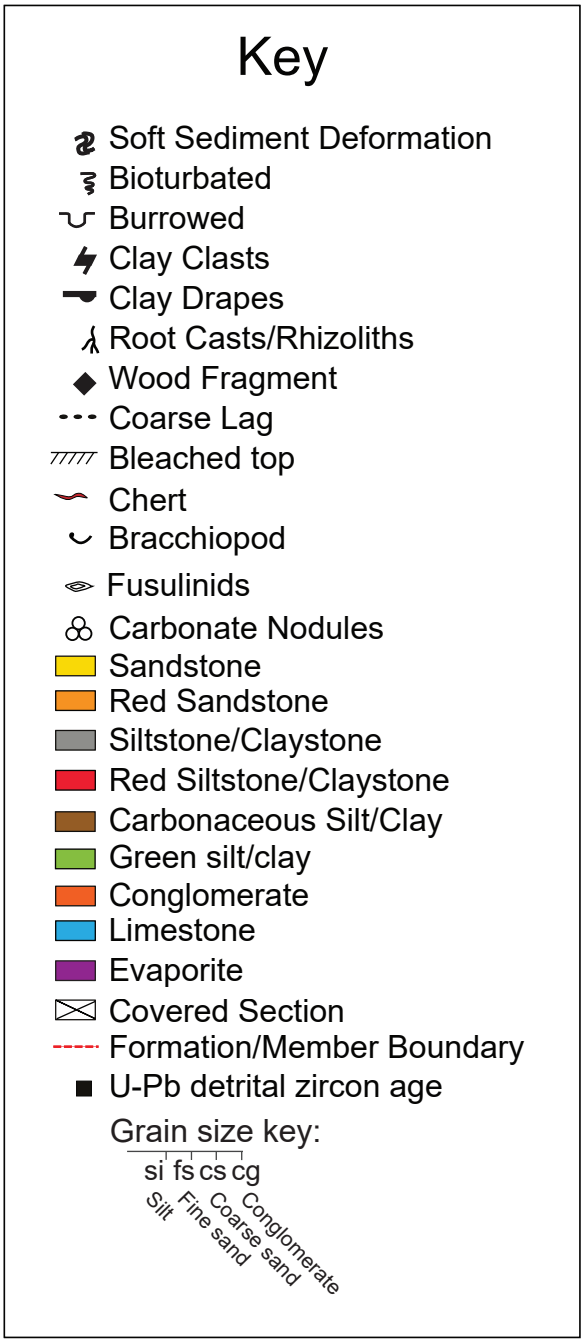

Supplemental Fig. 1. Measured section from the Sycamore Canyon section.

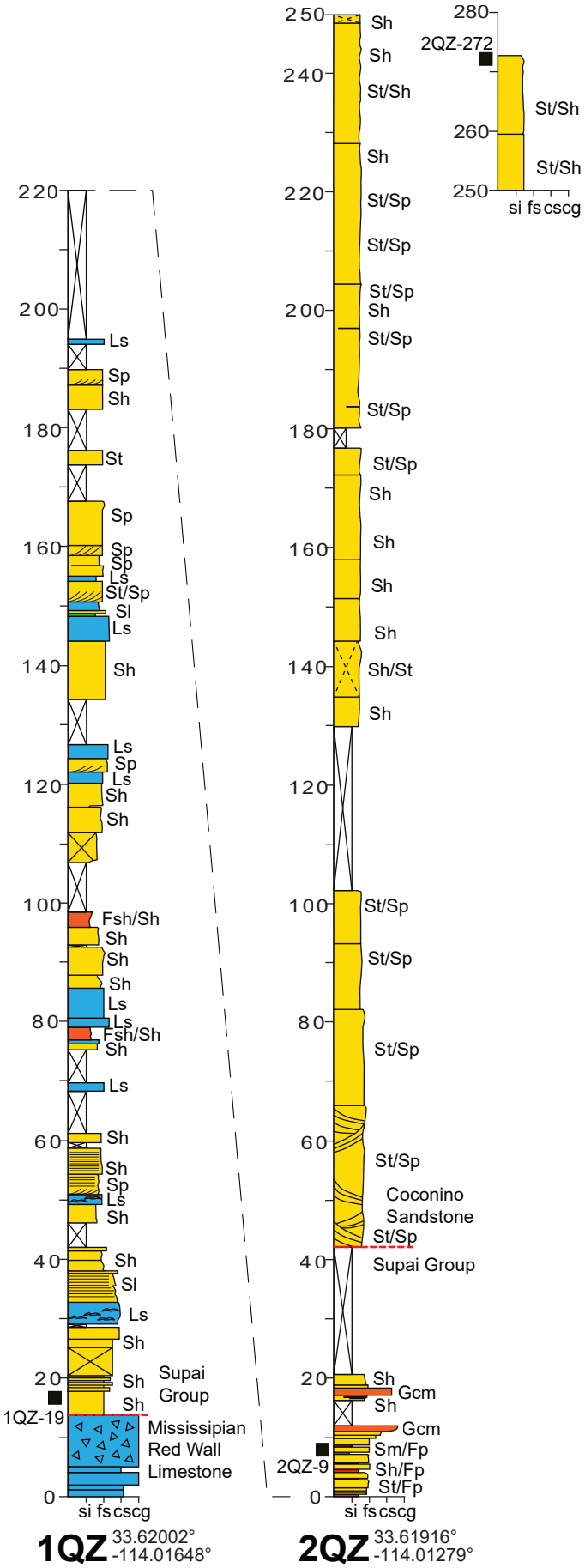

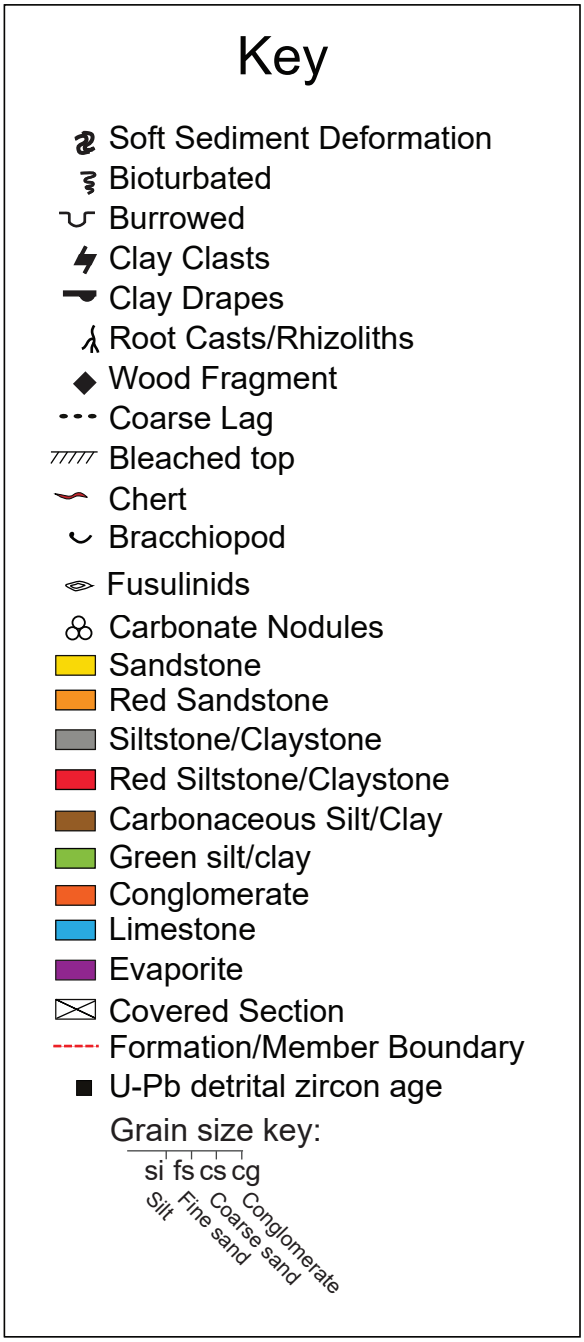

Supplemental Fig. 2. Measured Section from the southern Plomosa mountains.

Supplemental Fig. 3. Measured section from Mogollon Rim area near Payson, AZ. See Supplemental Fig. 1 for Key.

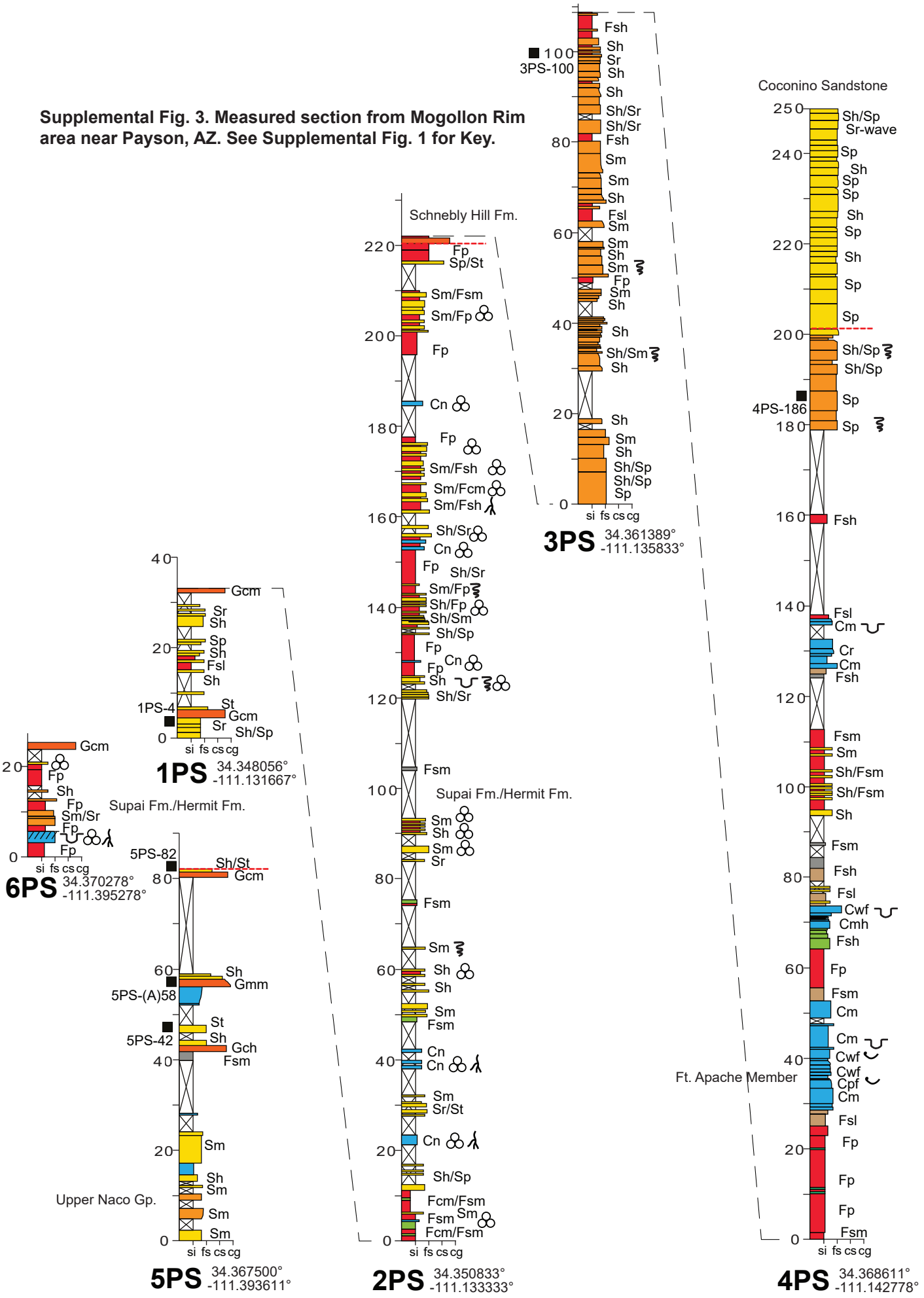

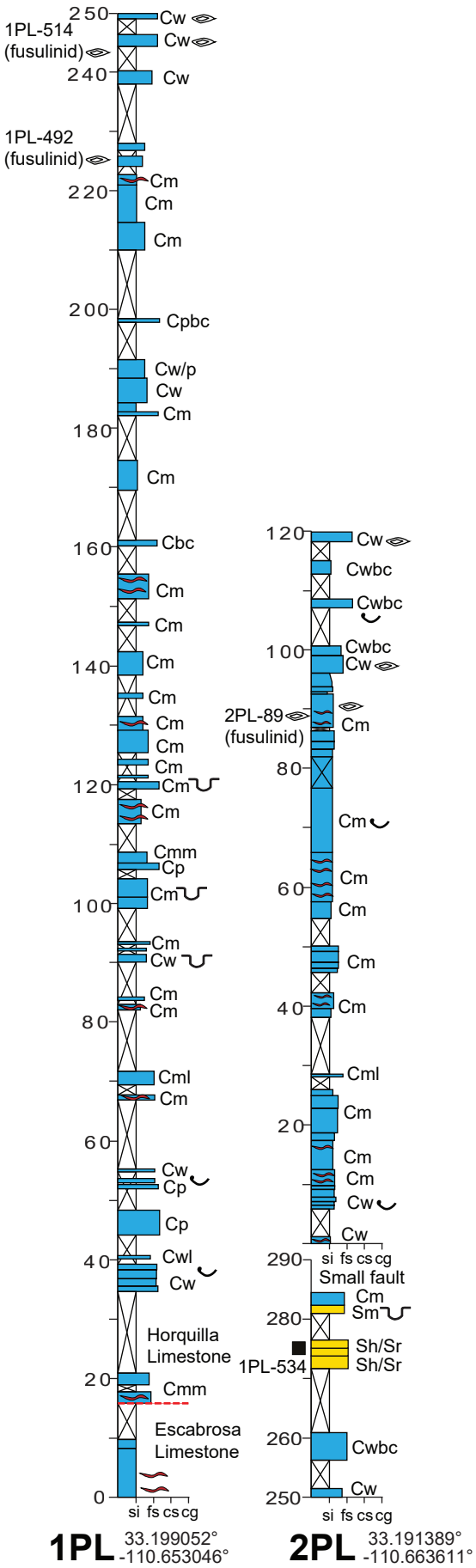

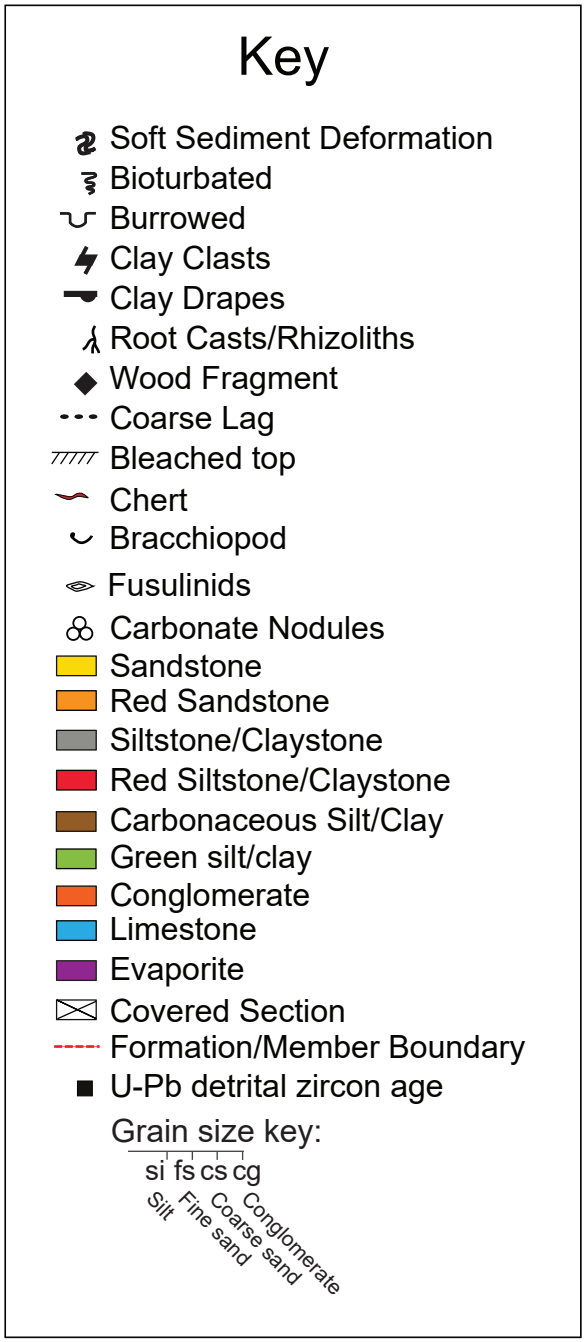

Supplemental Fig. 4. Measured section from the Mescal Mountains section.

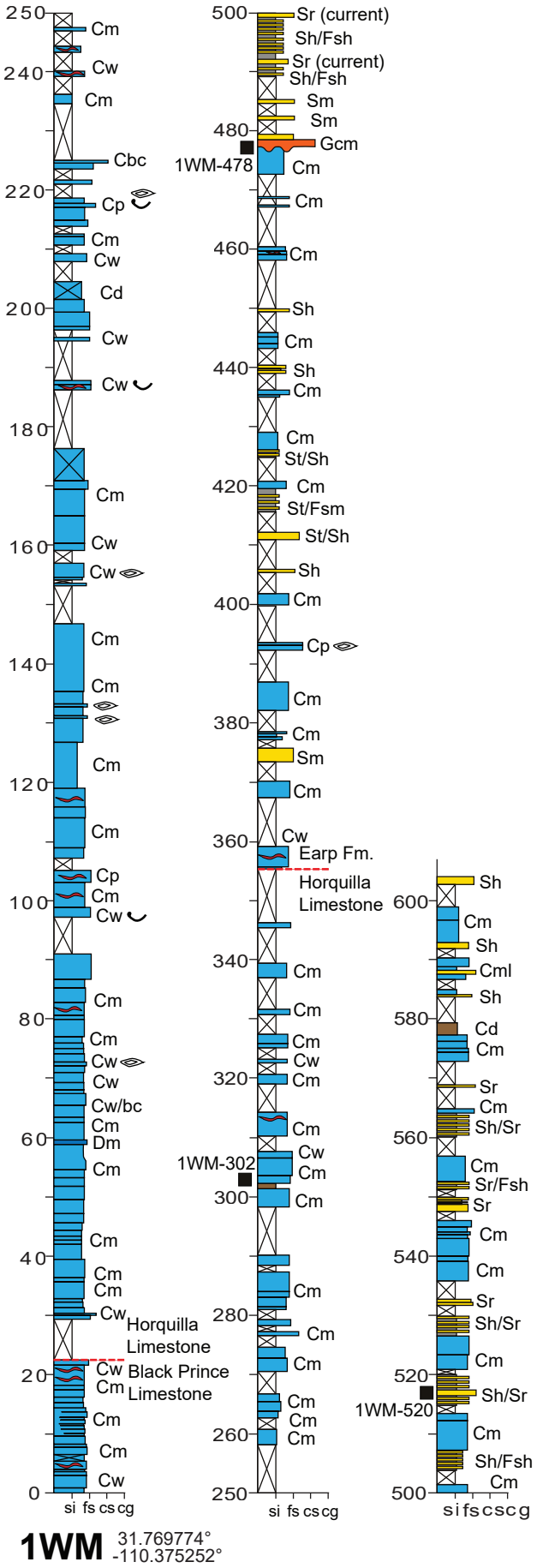

Key

- Soft Sediment Deformation
- Bioturbated
- Burrowed
- Clay Clasts
- Clay Drapes
- Root Casts/Rhizoliths
- Wood Fragment
- Coarse Lag
- Bleached top
- Chert
- Bracchiopod
- Fusulinids
- Carbonate Nodules
- Sandstone
- Red Sandstone
- Siltstone/Claystone
- Red Siltstone/Claystone
- Carbonaceous Silt/Clay
- Green silt/clay
- Conglomerate
- Limestone
- Evaporite
- Covered Section
- Formation/Member Boundary
- U-Pb detrital zircon age

Grain size key:

si fs cs cg

Silt, Fine sand, Coarse sand, Conglomerate

Supplemental Fig. 5. Measured section from the Whetstone Mountains section.

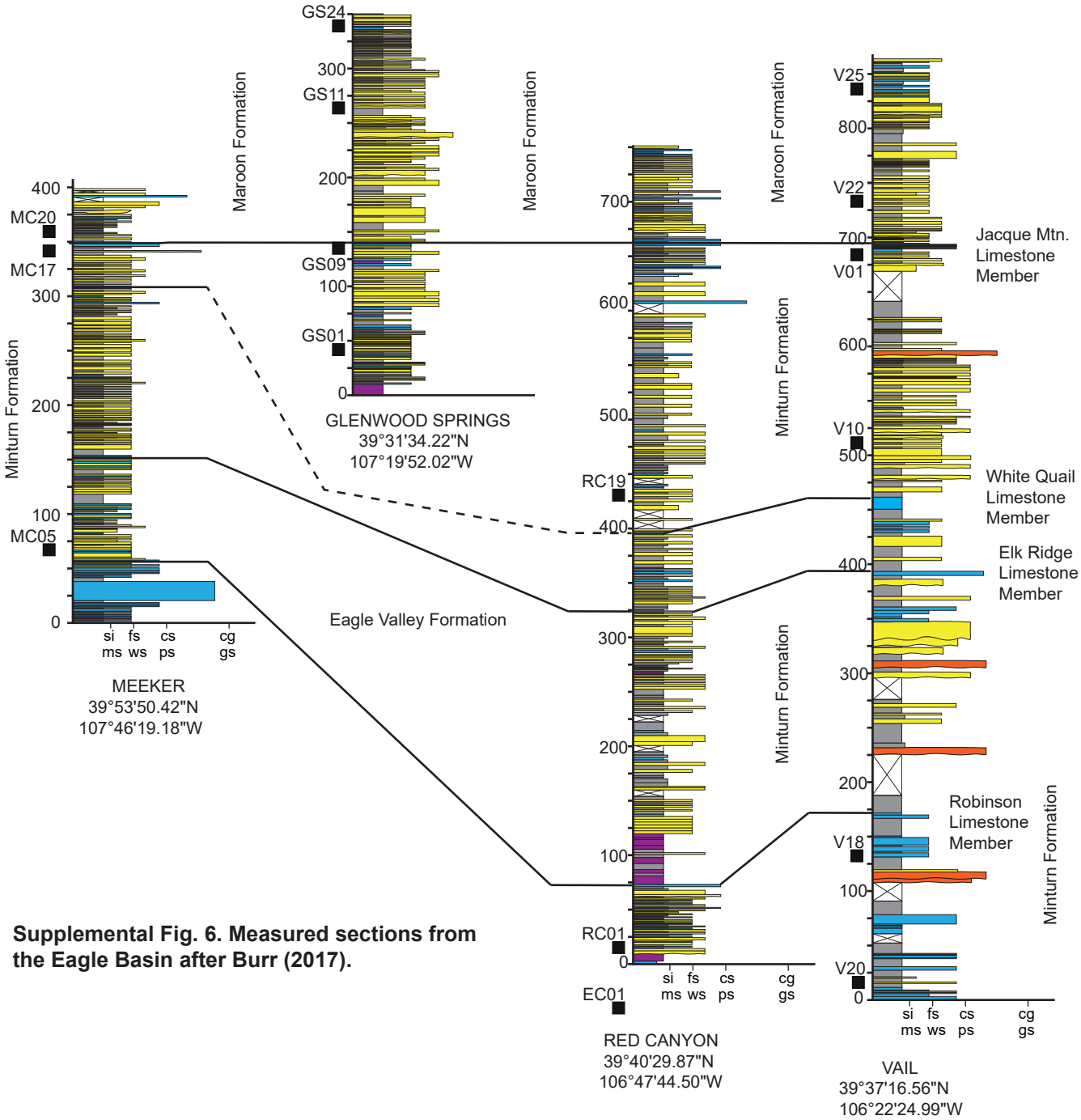

Supplemental Fig. 6. Measured sections from the Eagle Basin after Burr (2017).

TABLE 1. LITHOFACIES AND INTERPRETATIONS USED IN THIS STUDY†

Lithofacies Code	Description	Interpretation
Fsl	Laminated red, green, or gray siltstone	Suspension-settling in ponds and lakes
Fp	Massive, bioturbated, mottled siltstone, usually red; occasional carbonate nodules	Paleosols, usually calcic or vertic
Sm	Massive medium- to fine-grained sandstone; bioturbated	Bioturbated or pedoturbated sand, penecontemporaneous deformation
St	Medium- to very coarse grained sandstone with trough cross-stratification	Migration of large 3D ripples (dunes) under moderately powerful (40–100 cm/s), unidirectional flows in large channels
Sh	Fine- to medium-grained sandstone with plane-parallel lamination	Upper plane bed conditions under unidirectional flows, either strong (>100 cm/s) or very shallow
Gcm	Pebble to cobble conglomerate, moderately sorted, clast supported, unstratified, poorly organized	Depositition from sheetfloods and clast-rich debris flows
Gcm(i)	Pebble to cobble conglomerate, well sorted, clast supported, unstratified, imbricated (long axis transverse to paleoflow)	Depositition by traction currents in unsteady fluvial flows
Gch	Pebble to cobble conglomerate, well sorted, clast supported, horizontally stratified	Deposition from shallow traction currents in longitudinal bars and gravel sheets
Gch(i)	Pebble to cobble conglomerate, well sorted, clast supported, horizontally stratified, imbricated (long axis transverse to flow)	Deposition from shallow traction currents in longitudinal bars and gravel sheets
Cm	Carbonate mustone, massive	Low energy deposition, extensive bioturbation; deposition below storm wavebase
Cml	Carbonate mustone, laminated	Low energy deposition; limited to no benthic fauna; below SWB, possible anoxic conditions
Cw	Carbonate wackestone	Moderate energy enviroment; deposition below SWB to between SWB and FWWB
Cwl	Carbonate wackestone, laminated	Low energy deposition; below storm wavebase
Cp	Carbonate packstone	Moderate energy enviroment; deposition between SWB and FWWB
Cbc	Bioclastic packstone to grainstone	High energy environment; above FWWB
M	Mircitic massive gray and yellow marl	Lacustrine carbonate mudstone

†Siliciclastic facies after Miall (1978) and DeCelles et al. (2011); carbonate facies after Wilson (1975) and Bishop et al. (2010).